# NUMERICAL DETERMINATION OF SCATTERING AND BOUND STATES VIA SELF-CONSISTENT FIELD THEORY

by

MICAH TYLER

A DISSERTATION

Submitted in partial fulfillment of the requirements
for the degree of Doctor of Philosophy in the
Applied Mathematics Graduate Program
of Delaware State University

DOVER, DELAWARE
August 2019

This dissertation is approved by the following members of the Final Oral Review Committee:

Dr. Dawn A. Lott, Committee Chairperson, Department of Mathematical Sciences, Delaware State University

Dr. Fengshan Liu, Committee Member, Department of Mathematical Sciences, Delaware State University

Dr. Jinjie Liu, Committee Member, Department of Mathematical Sciences, Delaware State University

Dr. Matthew Tanzy, Committee Member, Department of Mathematical Sciences, Delaware State University

Dr. Essaid Zerrad, External Committee Member, Department of Physics and Delaware State University

# DEDICATION

This dissertation is dedicated to my parents, Stuart Tyler and Lisa Tyler. They have been the biggest influence in my life. I know they will do anything to insure my success and happiness. I appreciate all of the sacrifices they have made over the years. My success is an extension of their hard work.

# ACKNOWLEDGEMENTS

# Numerical Determination of Scattering and Bound States via Self-consistent Field Theory

Micah Tyler

Research Advisor: Dr. Dawn A. Lott

## ABSTRACT

Interpretation of atomic spectra and the applications of atomic spectroscopy to current problems in astrophysics, laser physics, and thermonuclear plasma require a precise knowledge of atomic structure and dynamics. The collisional excitation and ionization of atomic targets by electron impact is distinct in that one or more electrons are in the continua, which makes the theory complicated and also drastically disturbs the system for probing and detection.

Analysis of interacting atomic systems is complex and many approximate methods have been developed in the past. The most prominent of these methods is the Hartree-Fock procedure and its relativistic and multiconfiguration extensions. This self-consistent-field (SCF) approach has been limited to treating only fully bound, negative energy states whose corresponding wave functions are square-integrable. Recently, the SCF extension to scattering in which continuum (positive-energy) states are involved, has been formulated. The non-integrability of the continuum functions can be overcome by an amputation procedure that retains all of the physical essentials of the scattering system. It is extended here to the electron-hydrogenic scattering system in the zero angular momentum coupling models. In this project, the focus is on devising a numerical algorithm for solving such systems of integro-differential equations stemming from the SCF theory. The method is compared with

results obtained by several other approaches. It is shown that the newly devised numerical approach converges as the amputated continuum functions provide an effective projection of the scattering function.

# TABLE OF CONTENTS

# LIST OF TABLES

# LIST OF FIGURES AND ILLUSTRATIONS

# Chapter 1

# INTRODUCTION

In the infancy of the field of atomic physics, Joseph John Thomson [19] conducted a study with beams of negative particles. In 1897, these light-weight particles with negative charge became known as electrons. Early developments of atomic structures are still used today to conduct theoretical and experimental research. In the 1920s, the quantum model of an atom was birthed. Quantum theory is used to show how the wave behavior of electrons yields the quantized energy when electrons interact with the nucleus. By doing so, the electrons emit a set of discrete wavelengths.

The Schrödinger equation and perturbative methods are used to interpret the wavelengths and energies of the all the electrons in an atomic system approximately. In this dissertation, the Hartree-Fock Approximation (HFA) is utilized to represent a total wave function such that a single electron wave equation can be determined with the effect of an N-electron system. Numerical methods are applied to scattering and bound state wave functions to solve for energies of the electron.

Over the years, different methods were introduced to treat many-body systems to find the bound and scattering states. Most of these techniques were studies on specific atomic structures and then were generalized to extend to more complex systems. In this chapter, we will highlight some profound theories, numerical methods, and subroutines that have influenced the progression of atomic theory.

## 1.1 Close-Coupling Theory

The convergent close-coupling theory for atomic and molecular systems is based on a complete $L_2$ expansion of the total wave function in the Schrödinger equation for all energies for elastic, excitation, ionization and charge exchange process. Close-coupling methods give

approximation for quantum collision systems.

Burke et al. [13] investigated the scattering of electrons and positrons by atomic hydrogen for projectile energies. A close-coupling approximation was used to expand the total wave function in hydrogen eigenstates. Then, Burke et al. [12] calculated the following: differential and total cross sections for elastic and inelastic scattering, polarization and correlation of electron spin quantities, and the radiation emitted in various electrons due to polarization

Burke et al. [14] presented a six-state, close-coupling calculation of low-energy electron scattering by hydrogen. The first six hydrogen eigenstates of hydrogen were found by expansion and the remaining were solved computationally. Taylor and Burke [63] applied the same s-wave scattering of electron by atomic hydrogen to the correlation method. This method observed wave functions that were more flexible. The results were compared with the close-coupling results obtained with three states for the desired energy region and both methods were acceptable.

Bray and Stebovics [9] studied close-coupling for expanding the target state in an orthogonal $L_2$ Laguerre basis. This was not an approximation and convergence was achieved by increasing the basis size. This was studied on 2s and 2p differential cross-sections, spin asymmetries and angular correlation parameters for 2p excitation.

Bray [10] extended the close-coupling method to hydrogen-like targets, atoms or ions. The work treated H, Li, Na, K atoms, and many ions that have the same isoelectronic sequence as any of these atoms. The method's reliability is independent of the projectile energy and can be applied to a large set of measurements for electron scattering on sodium (Na). This includes the measurement of spin antisymmetries, singlet and triplet, reduced Stokes parameters, differential, integrated, and total cross-sections as well as the total ionization

2

spin asymmetry.

## 1.2 Variational Methods

The variational method finds the lowest expectation energy value which is the ground state energy. This procedure will give the best possible approximate wave function because it is closer to the true energy of the system.

Bransden et al. [7] applied a variational method to calculate phases for the s-wave and p-wave scattering of electron for the hydrogen atom. The study included full electron exchange and investigated polarization. John [34] applied the variational method used by Bransden to calculate the phases for s-, p- and d-waves analytically.

Schwartz [53] used the variational principle to calculate the s-wave elastic scattering of electrons from atomic hydrogen using trial functions introduced by Hylleraas [32] to describe bound states for two-electron atoms. The phase shifts were calculated and converged well at energy levels up to 10 electron volts. Keeping the energy level in the range left residual uncertainties less than one thousandth of a radian. Accurate values were determined for the scattering lengths.

Armour et al. [4] discussed accurate calculations of low-energy scattering for hydrogen and helium atoms and the hydrogen molecule. The variational method and trial functions that contain Hylleraas-type correlation terms were used for these atomic structures. Positronium formation in the Öre gap was taken into account for hydrogen. Methods were discussed to extend these calculations to electron-helium.

## 1.3 R-matrix Method

The R-matrix method was first presented by Wigner and Eisenbud [65] for nuclear reactions. Burke and Robb [15] extended the method to study low energy scattering by

complex atoms and ions in 1971 and many others have made improvements for this method.

Burke and Robb [15] used the R-matrix method to calculate the elastic scattering of electrons by hydrogen and helium atom. The phase shifts for electron-hydrogen were obtained in the static approximation and this allowed atomic polarizability by using the pseudo-state method. Electron-helium scattering phase shifts were obtained using Hatree-Fock and a correlated target wave function. The phase shift was dependent on the number of basis states included in the expansion of the total wave function.

Burke et al. [16] developed a R-matrix theory of electron-atom and electron-molecule scattering at intermediate energies. The outer valence electron of the target atom or molecule and the scattered electron were expanded in terms of a continuum R-matrix basis. This enabled target eigenstates as well as pseudostates representing inelastic effects to be accurately represented in an internal region. A two-dimensional R-matrix propagator approach was developed that enabled the internal region to be subdivided and highly excited target states that extend out to large distances to be treated. This theory was combined with the T-matrix energy averaging technique. This method produced accurate cross-sections at intermediate energies. The method was illustrated by applying it to the elastic s-wave scattering of electrons by atomic hydrogen from threshold to 60 eV.

Scholz and Burke [52] discovered accurate calculations of new intermediate energies using the R-matrix theory for electron-hydrogen scattering. Cross-sections for elastic scattering and 1s-2s and 1s-2p excitation processes were presented for s-, p-, and d- partial-wave symmetries. Phase shifts and resonance positions and widths are below n=2 threshold.

Scott and Burke [54] developed a reduced intermediate energy R-matrix approach to allow more rapid calculation of accurate cross-sections at intermediate energies. The approach was applied to electron-hydrogen atom scattering for $L = 0$ (angular momentum),

S=0 (total spin) and even parity to give the first accurate cross-section for $n = 1$ and $n = 2$ to $n = 3$ transition at intermediate energies.

## 1.4 Numerical methods

In this section we discuss a variety of numerical methods that have been used to solve atomic systems and collisions.

### 1.4.1 Noniterative Methods

Sams and Kouri [50] introduced an integral equation method to solve collision problems for homogeneous integral solutions. The method was noniterative and was applied well to local and non-local interactions. The study was extended to solve integral equations of scattering coupled channels [51].

Smith and Henry [62] applied the non-iterative integral equation theory to open and closed channels with exchange and orthogonality was formulated for the multi-channel scattering. This method solves coupled, integro-differential equations of the scattering problem from zero out to some transformation point where the reactant matrix is projected out to its asymptotic value by using a matrizant technique.

Botero and Sherzter [6] used a direct numerical solution of the Schrödinger equation for quantum scattering problems. Each partial wave function was expanded in coupled spherical harmonics. The corresponding radial functions were expanded in a local basis set using finite-element analysis with appropriate scattering boundary conditions for s, p, d, and f-elastic phase shift of electron-hydrogen.

Simos et al. [58] developed a two-step method for computing eigenvalues and resonances of the radial Schrödinger equation. Numerical results were obtained for the integration of the eigenvalue and the resonance problems. This new method was shown to be better than

similar method by using several potentials.

Simos [59] studied the importance of the properties of P-stability and Trigonometric-fitting for the numerical integration of the one-dimensional Schrödinger equation. This was done through the error analysis and the application of the studied methods to the numerical solution of the radial Schrödinger equation.

### 1.4.2 Iterative Methods

Poet [42] problem solved for low and medium energies by neglecting all angular momentum for simplified electron-hydrogen excitation. The integrals arising were expressed in terms of hypergeometric functions, so that accurate solutions could be computed rapidly. The model included an effect that is more complex than realistic problems. Issues were the strong coupling between an infinite number of open channels and need for an adequate continuum representation.

Ixaru [33] found expressions for the coefficients of the Numerov scheme to ensure the optimal approximation to the Schrödinger equation in the deep continuum spectrum of energies.

Poet [43] presented a new method for obtaining scattering information for electron-atom and ion collisions. Results were obtained for model electron-hydrogen collisions when the angular momentum is neglected. Schrodinger's equation was separable in the outer region, so that the wave function is a linear sum of Coulomb functions multiplied by exponentials. An explicit interpolation scheme was used for the generalized unitary matrix, thus eliminating any ill-conditioning. This scheme converged rapidly. Five adjustable parameters gave errors of around 1-2 percent for incident energies of 0.8 to 3 Rydberg. The results were obtained by using a separable pseudo-state expansion in the outer region.

Raptis [45, 46] implemented multi-step methods to solve the Schrödinger equation without exchange. The Chebyshevian Multi-step Theory of Lyche [39] was developed and applied to the numerical solution of the radial form of the Schrödinger equation. Significant improvements were made over previously reported approaches.

Berghe et al. [5] revisited an algorithm previously introduced by Brown et al. (1963) [8] for solving radial Schrödinger equations that was implemented in a more accurate way. The method was applied to equations where potentials were finite at the origin and have an asymptotic behaviour $V(r) \to 0$ as $r \to \infty$. The method was used for many potentials as well as Coulomb-like potentials. Comparisons were made with approximate methods and exact bound state energies.

Simos [57] developed a new four-step exponentially-fitted method. The expressions for the coefficients of the method were found to ensure the optimal approximation to the eigenvalue Schrödinger equation for positive energy.

Kim [36] presented the Lanczos [37] method for a non-local optical model calculation of the Schrödinger equation. The method was tested with other methods and adapts well to solving large dimensional, coupled channel equations very efficiently.

Bray [11] discovered a way to apply the convergent close-coupling method to allow the continuum to be treated in a systematic manner by using square-integrable states. The convergent close-coupling method used an expansion of the target in a complete set of orthogonal $L_2$ functions to form a basis for the underlying Hilbert space. To demonstrate convergence in the scattering amplitudes of interest, the basis size is increased.

Waxman [64] used numerical methods to find accurate determinations of the bound-state eigenfunctions and eigenvalues of a differential operator such as the one-particle Schrödinger Hamiltonian. The method applied potentials that asymptotically vanish. The eigenvalues

and eigenfunctions were determined as functions of the strength of the potential and this allowed for the determination of the bound-state energies for arbitrarily weak strengths of the potential. Since the matrix was not diagonalized, the method could be applied to problems with space dimension greater than unity.

Rawitscher et al. [47] extended the spectral non-iterative method that was previously designed to solve the Lippmann Schwinger integral equation with local potentials, to include the exchange non-locality. It was applied to the electron-hydrogen scattering case where the bound electron remains in the ground state and the incident electron has zero angular momentum.

Shao et al. [56] introduced an algorithm to calculate the Green's function of the Schrödinger equation in a block layered potential. Applying the block layered potential has many applications in quantum modeling of electron transport. The method is based on expanding the eigenfunction of a Sturm-Liouville problem and a collocation matching procedure.

Anastassi [1] introduced a new methodology for the construction of numerical methods for the approximate solution of the one-dimensional Schrödinger equation. The new methodology was based on the requirement of vanishing the phase-lag and its derivatives. The efficiency of the new methodology was proved through error analysis and numerical applications.

Simos [60] developed new methodology of efficient numerical methods for the approximate the one-dimensional Schrödinger equation. This methodology was based on the phase-lag and its derivatives vanishing. Error analysis and numerical results were used to validate this methodology.

Pillai [41] recasted the well-known Numerov method for solving Schrödingers equa-

tion into a representation of the kinetic energy operator on a discrete lattice. A high-level programming environment made it simple to calculate and plot accurate eigenvalues and eigenvectors for a variety of potential problems. Their paper illustrated the method by calculating high-accuracy solutions for the $|x|$ potential.

Nikolopoulos [40] developed a calculational method of solving the scattering equations for spherically symmetric potentials by expanding the solutions on Coulomb functions. A multistep integration scheme together with the standard partial wave analysis in a region where the potential term dominates were utilized. The method is applied to any physical problem scattering equation without exchange terms. A two-step Coulomb-fitted integration scheme by calculating the short-range scattering phase shifts for various potentials were demonstrated in this research.

Arellano et al. [2] presented an exact solution for the scattering wave function from a non-local potential in the presence of Coulomb interaction. The approach was based on the construction of a Coulomb Green's function in coordinate space whose associated kernel involves any non-local optical potential superposed to the Coulomb-screened interaction. The scattering wave function, exact solution of the integro-differential Schrödingers equation posed no restrictions on the type of non-locality of the interaction.

## 1.5 Subroutines

In recent years, subroutines have been created for public use to solve atomic systems. These subroutines address specific problems and require certain parameters. Here, we review some of the subroutines that are available, and the type of problem they can solve.

Seaton [55] used the code NUMER for numerical integrations of Coulomb radial wave functions using the Numerov method. The inputs required were a function and its derivative

to start integration, an integration range and an accuracy parameter, abdominal circumference, such that the accumulated error is no larger than abdominal circumference. Alternative inputs were initial function, integration step, and function after first step. The program is suitable for positive energies.

Čertík et al. [17] presented a robust and general solver for the radial Schrödinger, Dirac, and Kohn-Sham equations. This solution used general potentials and meshes: uniform, exponential, or other defined by nodal distribution and derivative functions. For a given mesh type, convergence was controlled systematically by increasing the number of grid points. Radial integrations were carried out using a combination of asymptotic forms, Runge-Kutta, and implicit Adams methods. Eigenfunctions were determined by a combination of bisection and perturbation methods for robustness and speed. An outward Poisson integration was employed to increase accuracy in the core region, allowing absolute accuracies of 108 Hartree to be attained for total energies of heavy atoms, such as uranium. Detailed convergence studies were presented, and computational parameters were provided to achieve accuracies commonly required in practice. Comparisons to analytic and current-benchmark density-functional results for atomic numbers Z=1 to 92 were presented, verifying and providing a refinement to current benchmarks. An efficient, modular Fortran 95 implementation, "dftatom," was provided as open source, including examples, tests, and wrappers for interface to other languages; wherein particular emphasis is placed on the independence, reusability, and generality of the individual routines.

Salvat et al. [48, 49] described a Fortran package of subroutines RADIAL for the numerical solutions of the Schrödinger wave equation of electrons in central potentials. This includes finite-range potentials as well as combinations of Coulomb and finite-range potentials. The function $V(r)$ was used calculate the natural cubic spline that interpolates a table

of values provided by the user. The radial equations were solved by using piecewise exact power series expansions of the radial functions, which are summed up to the prescribed accuracy so that truncation errors can be completely avoided. The RADIAL subroutines computed radial wave functions, eigenvalues for bound states and phase shifts for free states. These subroutines compute the radial functions and phase shifts for free states of complex optical potentials having a finite-range absorptive imaginary part. The subroutines provided example main programs, as well as specific programs that perform calculations relevant in atomic, nuclear, and radiation physics that involve the self-consistent solution of the Dirac-Hartee-Fock-Slater equations for neutral atoms and positive ions, and the calculation of cross-sections for elastic scattering of high-energy electrons and positrons by atoms and of nucleons by nuclei. The distribution package gave a detailed manual with a description of the basic physics and the mathematical formulas implemented in the subroutines.

## 1.6 Hartree-Fock Approximation and Numerical Methods

The first study of the Hartree-Fock (HF) method was introduced by Hartree [29, 30] in the 1920s. Since then, many developments have been made to improve the theory and make it a popular approximation method for atomic spectra. This dissertation will focus on this self-consistent approach to approximating scattering and bound state wave equations and numerical methods to solve these equations. In this section, we highlight some the contributions made over the years.

Fonte et al. [20] used the Newton iteration method for constructing a solution of the atomic and nuclear HF equations for an arbitrary number of particles. This was based on the theorem by Kantorovich [35] and the following points: 1) the two-body potential must be bounded; 2) the approximation used to start the iteration sequence must satisfy certain

conditions for local and nonlocal potentials.

Slater [61] showed that the HF equation can be regarded as the Schrödinger equations for the motion of electrons. Each electron moves in a slightly differential potential field that is computed by electrostatics of all the charges of the system. A weighted mean potential was investigated for all electrons. The weighted mean potential was a simplification of the HF method and pictorially agreed with solid states.

Lieb and Simon [38] proved the existence of solutions of the HF equations which minimize the HF energy for neutral atoms and molecules and positive ions. They established some properties of the solutions including exponential falloff.

Hahn [26, 27] improved on the conventional HF and HF Approximations for electron-bound systems to treat positive-energy scattering problems. This was achieved by using square-integrable functions associated with the scattering wave functions and relaxing the asymptotic condition. This method differs from previous methods because it can treat both the bound and scattering orbitals simultaneously. It also improved the wave function systematically through configuration interaction. In 2014, Hahn [28] discussed the self-consistent field theory of collisions and how they were formed by incorporating the unique dynamics generated by the self-averaged potentials. Alternatively, the integrable spin orbitals were generated by constructing the individual orbital equations that contain asymptotic sources and self-averaged potentials. The orbital energies were not determined by the equations, and a special channel energy fixing procedure was developed to secure the solutions. It was also shown that the variational construction of the orbital equations has intrinsic ambiguities that were generally associated with the self-consistent approach. When a small subset of open channels were included in the source term, the solutions were only partially integrable, but the individual open channels were then treated more simply by properly selecting the orbital

energies. The configuration mixing and channel coupling were then necessary to complete the solution. The new theory improved the earlier continuum HF model.

Zerrad et al. [67] continued the self-consistent field (SCF) study and the results showed that the theory converges to the correct amplitudes and the exact boundary conditions when more configurations are added. Amputated wave functions and the weak asymptotic condition upon which the SCF theory is based, is justified as the weak asymptotic condition converges to the correct limit. It was then applied to the positron-helium and electron-helium scattering systems where the helium function was calculated simultaneously together with the scattering function. The phase shifts and the SCF target functions were compared with those obtained with the predetermined target functions in the conventional approaches.

Zerrad el at. [68] created a new numerical method for solving the integro-differential equations that appear in the theory of atomic scattering. The method decomposes the kernel into separable terms using the singular-value decomposition. A set of integro-differential equations has a residual integral kernel that is solved to obtain the wave function. From the wave function, the phase shift is evaluated. In 2009, Zerrad et al. [69] applied this method to low energy helium and illustrated how the Green's function for a Schrödinger equation with both local and non-local but fully separable potentials can be obtained without much difficulty by adding solution dependent constants to the Green's function distorted only by the local potential.

This dissertation is an extension of previous SCF work on numerical methods of scattering and bound states. Chapter 2 discusses the HF theory that produces the wave functions in a SCF and the application of the theory to atomic structures that is used in later chapters. In Chapter 3, Numerov's method is used to find the scattering wave function and phase angle. Chapter 4 discusses the Green's function and SVD method to separate the non-local

kernel and discovery of more solutions at low energies for the hydrogen atom. In Chapter 5, an energy matching scheme for the solution of the eigenvalue radial problem for bound state electrons is investigated. The HF Theory that was introduced by Hahn to treat scattering problems is used to solve for the scattering and bound orbitals simultaneously in Chapter 6. These states are computed using the numerical methods in the preceding chapters. Chapter 7 contains a conclusion of the findings. Future work will presented in Chapter 8.

# Chapter 2

# HARTREE-FOCK APPROXIMATION

## 2.1 Overview

The Hartree-Fock Approximation (HFA) is used to find approximate solutions to many-body problems for atoms, molecules and solids. With the HFA, single particle states can be found based on the effect of the multi-particle system. This method is used to access atomic collision and give an accurate view of the atomic structure with many electrons. For many-body problems, this approximation has many real-world applications and is easily applied to numerical computations. In this chapter, a general overview of theory of the Hartree-Fock (HF) method is given, as well as, applications of the theory for the hydrogen atom.

## 2.2 Theory

In this section, a many body system will be applied to the HFA. This general form can be extended to more complex systems. The many body, time-independent system is governed by the Schrödinger equation,

$$\hat{H}\Psi = E\Psi \tag{2.1}$$

where $\Psi$ is the total wave function

$$\Psi(x_1, x_2, ..., x_N). \tag{2.2}$$

The Hamiltonian for a molecular system composed of $M$ nuclei with charge $Z_\alpha$ and position $R_\alpha$ and $N$ electrons can be written as

$$\hat{H} = -\sum_{j=1}^{N} \left( -\frac{1}{2} \bigtriangledown_{x_j} + \sum_{\alpha=1}^{M} \frac{Z_\alpha}{|R_\alpha - x_j|} \right) + \sum_{i,j=1}^{N} \frac{1}{|x_1 - x_j|}, \tag{2.3}$$

where the first term represents the kinetic energy with respect to the the $x_j$ electron. The second term describes the attraction of the nuclei to the jth electron. The final term represent the interactions of all the electrons which has repulsive characteristics. The Hamiltonian is the total energy of the system.

In quantum mechanics the position and momentum of an electron cannot be determined at the same time. This phenomenon is based on the Heisenberg Uncertainty Principle [18, 21, 22, 25]. The wave function $\Psi$ is used to describe the quantum state of the electrons. The probability distribution of finding the electron at a position $x$ is based on the modulus of the wave function $|\Psi|^2$. The description of the system is intrinsically probabilistic [18, 21, 22, 25]. The energy of the system is obtained by taking the scalar product of

$$E\Psi = \left\langle \Psi | \hat{H} | \Psi \right\rangle = \int_{\mathbb{R}^3} \Psi(x_1, ...x_N) \hat{H} \Psi(x_1, ...x_N) dx_1, ..., dx_N. \tag{2.4}$$

The ground state of the system is given by minimizing the wave function of the energy. This means that wave function must be anti-symmetric and the norm of the wave function must be 1. The product form of the total wave function is called the Hartree Product. It is written as

$$\Psi(1, 2, ..., N) \simeq \Psi_{HF}(1, 2, ..., N) = \psi_1(\mathbf{r}_1)\psi_2(\mathbf{r}_2)...\psi_N(\mathbf{r}_N). \tag{2.5}$$

The wave function contains the product of the orbitals $\psi$. These orbitals describe the wave

behavior of the N-electrons in the system.

The total wave function does not account for the energy exchange of the electrons. According to quantum theory, this not an accurate representation of the electrons in a atomic system. The HFA assumes that each electron moves in an averaged potential based on the other electrons. The wave function needs to be anti-symmetric to take into account that any two electron are indistinguishable [18, 21, 22, 25]. The wave function should be written as

$$\Psi(1, ..., i, j, ..., N) = -\Psi(1, ..., j, i, ..., N). \tag{2.6}$$

This property comes form the Pauli Exclusion Principle [18, 21, 22, 25]. To produce all possible wave functions of a many body problem, a permutation operator is applied to the total wave function. The anti-symmetric form of the wave function is written as

$$P_{ij}\Psi(1, ..., i, j, ..., N) \tag{2.7}$$

where $1 \leq (i, j) \leq N$ and $i \neq j$. This operator addresses the intrinsic spin coordinates that insures there are two spin-orbitals for each spatial orbital. These spin orbitals have opposite signs. The wave function is rewritten simply as function $\mathbf{x}$ of spatial $\mathbf{r}$ and spin coordinates $\omega$. Due to spin-degeneracy, it is more convenient to continue with the spatial components only. Assuming the HFA can be expressed as a Slater determinate of single particle wave functions will allow anti-symmetry for a N-electron system [18, 21, 22, 25]. This can be

simply written as

$$
= \frac{1}{\sqrt{N!}}
\begin{vmatrix}
\psi_1(\mathbf{r}_1) & \psi_2(\mathbf{r}_1) & \cdots & \psi_N(\mathbf{r}_1) \\
\psi_1(\mathbf{r}_2) & \psi_2(\mathbf{r}_2) & \cdots & \psi_N(\mathbf{r}_2) \\
\vdots & \vdots & \ddots & \vdots \\
\psi_1(\mathbf{r}_N) & \psi_2(\mathbf{r}_N) & \cdots & \psi_N(\mathbf{r}_N)
\end{vmatrix}
$$

$$
= \frac{1}{\sqrt{N!}} \sum (-1)^{p_n} P_n x_1(1) x_2(2) x_N(N)
$$

The Slater determinate accounts for all $N!$ permutations of the N single particle states of the total wave function. The value $p_n$ depends on whether the permutation $P_n$ is even or odd. This process allows the many body problem to be decoupled and leaves a single-particle wave function that is based on a self- consistent field.

## 2.3 Hartree Product and Applications of the Hartree-Fock Approximations

Now that the each particle in a N-electron system can be obtained using HFA, this dissertation will look at specific atomic collisions and systems. Then numerical methods are applied to determine the energies of the electronic particles. There are not many analytic solutions to these type of problems. Hence, this research looks at atomic collisions and systems with known analytic solutions. The hydrogen atom has well known analytic solutions that will be used to compare with numerical solutions found in this dissertation. This section will discuss the different interactions that can be applied to the hydrogen atom. Specifically, single channel configuration of the bound and scattering states will be evaluated. These simple cases are the stepping stone to more complex atomic structures.

### 2.3.1 Scattering Wave Equation for Positron-Hydrogen Scattering System

The equation below describes a hydrogen-like atomic system with two particles, where the electron particle is bound to the nucleus, and the incident particle is a positron. Since the incident particle is a positron, it has a positive charge which makes it distinguishable from the electron. This means there is no exchange of energy between the particles. The hydrogen-like system without exchange is the following 3-dimensional Schrödinger equation:

$$-\frac{\hbar^2}{2\mu}\left(\nabla^2_{\mathbf{x}_1} + \nabla^2_{\mathbf{x}_2}\right) - \left[+\frac{Ze^2}{\mathbf{x}_1} - \frac{Ze^2}{\mathbf{x}_2} + \frac{e^2}{\mathbf{x}_>}\right]\Psi(\mathbf{x}_1, \mathbf{x}_2) = \bar{E}\Psi(\mathbf{x}_1, \mathbf{x}_2). \qquad (2.8)$$

where $Z$ is the charge of the nucleus. The kinetic energy $(\bar{E}_k)$ of the incident electron acts on the ground state of the system. The overall wave function of the system is denoted $\Psi(\mathbf{x}_1, \mathbf{x}_2)$. The total energy is $\bar{E}$. The charge of the particles is $e$ where the positron has a positive sign and the electron has a negative sign to indicate their respective charges. The reduced mass of the incident electron is $\mu$. The Planck's constant is $\hbar$. The position vectors of the electron and positron are denoted are denoted $\mathbf{x}_1$ and $\mathbf{x}_2$, and $\mathbf{x}_>$ is the distance between the two particles. To transform the variables into atomic units, multiply equation (2.8) by the quantity $\left(\frac{2\mu a_o^2}{\hbar^2}\right)$, where $a_o\left(\frac{\hbar^2}{2\mu e^2}\right)$ is the Bohr unit of length. The resulting equation is

$$\left[-\nabla^2_{\mathbf{r}_1} - \nabla^2_{r_2} - \frac{2Z}{\mathbf{r}_1} + \frac{2Z}{\mathbf{r}_2} - \frac{2}{\mathbf{r}_>}\right]\Psi(\mathbf{r}_1, \mathbf{r}_2) = E\Psi(\mathbf{r}_1, \mathbf{r}_2). \qquad (2.9)$$

Here $\mathbf{r} = \mathbf{x}/a_o$ is a displacement vector in units of Bohr, and $E = \bar{E}/\Re$ is the total energy in Bohr units. One Rydberg equal is to $\Re = \hbar^2/(2\mu a_o^2)$. We utilize the well-known

expansion $\frac{1}{r_>} \to \frac{1}{r_{12}}$ where

$$
\mathbf{r}_{12} = \begin{cases} \mathbf{r}_2 & \text{for } \mathbf{r}_1 \le \mathbf{r}_2 \\ \mathbf{r}_1 & \text{for } \mathbf{r}_1 > \mathbf{r}_2. \end{cases} \quad [3] \tag{2.10}
$$

The Hartee-Fock Approximation (HFA) expands the total wave function in terms of the bound states $\phi_i$ of the atomic electron and $\psi_i$ are the wave functions of the scattered positron in channel $i$, to be determined from the solution of a set of coupled equations. In this case, HFA without exchange terms is used to arrive at the homogeneous, ordinary differential equation governing the scattering wave function. The HFA without exchange is [23, 24]

$$
\Psi(\mathbf{r}_1, \mathbf{r}_2) = \sum_{i=1} \phi_i(\mathbf{r}_1)\psi_i(\mathbf{r}_2). \tag{2.11}
$$

The subscript $i$ represents the set of all quantum numbers which label the electron bound states. The corresponding principal quantum number is $n_i$, and the corresponding bound state energy is

$$
E_{B_i} = -\left(\frac{Z^2}{n_i^2}\right)\Re. \tag{2.12}
$$

In this dissertation, the ground state will be assumed, i.e., $i = 1$, and this subscript will be left off for simplicity, and $Z = 1$. With these assumptions the bound-state electron energy is $E_B = -\Re$ where $\Re$ is the Rydberg constant for hydrogen, and the incident electron has the asymptotic kinetic energy $\bar{E}_k = \bar{E} - E_B$. Assuming this is a positive quantity, $\bar{E}_k = E_C\Re$, where $E_C = k^2$, and the corresponding wave number $k$ in atomic units is given by

$$
E_C = \frac{\bar{E} - E_B}{\Re} = \frac{\bar{E} - (-\Re)}{\Re} = E + 1. \tag{2.13}
$$

based on equation (2.13), the bound state energy in this system is -1, and it will be labeled

as $E_B$ in all calculations of the atomic equations to reference in proceeding chapters.

The equation for $\psi$ is obtained by truncating the sum in equation (2.11) to one term, and inserting it into equation (2.9). Then, we multiply on the left by the functions $\phi = \phi_i(\mathbf{r}_1)$, and integrate over $d^3\mathbf{r}_1$.

$$\int \phi(\mathbf{r}_1) \left[ -\nabla^2_{\mathbf{r}_1} - \nabla^2_{\mathbf{r}_2} - \frac{2}{\mathbf{r}_1} + \frac{2}{\mathbf{r}_2} - \frac{2}{\mathbf{r}_{12}} - E \right] \phi(\mathbf{r}_1)\psi(\mathbf{r}_2)d^3\mathbf{r}_1 = 0. \qquad (2.14)$$

Then we have

$$\int \phi(\mathbf{r}_1) \left\{ -\nabla^2_{\mathbf{r}_1} - \nabla^2_{\mathbf{r}_2} - \frac{2}{\mathbf{r}_1} + \frac{2}{\mathbf{r}_2} - \frac{2}{\mathbf{r}_{12}} - E_C - E_B \right\} \phi(\mathbf{r}_1)\psi(\mathbf{r}_2)d^3\mathbf{r}_1 = 0.$$

$$(2.15)$$

Now the integral is separated by the desired wave equation and the Weak Asymptotic Condition (WAC) is enforced. Hence,

$$\int \phi(\mathbf{r}_1) \left\{ -\nabla^2_{\mathbf{r}_2} - \frac{2}{\mathbf{r}_2} - \frac{2}{\mathbf{r}_{12}} - E_C \right\} \phi(\mathbf{r}_1)\psi(\mathbf{r}_2)d^3\mathbf{r}_1$$
$$+ \int \phi(\mathbf{r}_1) \left\{ -\nabla^2_{\mathbf{r}_1} - \frac{2}{\mathbf{r}_1} - E_B \right\} \phi(\mathbf{r}_1)\psi(\mathbf{r}_2)d^3\mathbf{r}_2 = 0. \qquad (2.16)$$

The WAC is

$$\left\{ -\nabla^2_{\mathbf{r}_1} - \frac{2}{\mathbf{r}_1} - E_B \right\} \phi(\mathbf{r}_1) = 0. \qquad (2.17)$$

This condition is imposed to maintain the self consistent field, and the chosen energy of the

incident particle ($E_C$). Once the weak asymptotic condition is applied, the equation becomes

$$\left\{ -\nabla_{\mathbf{r}_2}^2 \left\langle \phi(\mathbf{r}_1) \middle| \phi(\mathbf{r}_1) \right\rangle - \frac{2}{\mathbf{r}_2} \left\langle \phi(\mathbf{r}_1) | \phi(\mathbf{r}_1) \right\rangle \right.$$
$$\left. + \left\langle \phi(\mathbf{r}_1) \frac{2}{\mathbf{r}_{12}} \phi(\mathbf{r}_1) \right\rangle - E_C \left\langle \phi(\mathbf{r}_1) | \phi(\mathbf{r}_1) \right\rangle \right\} \psi(\mathbf{r}_2) = 0. \tag{2.18}$$

For simplicity, the equation is rewritten as

$$\left\{ -\nabla_{\mathbf{r}_2}^2 A - \frac{2}{\mathbf{r}_2} A + B - E_C A \right\} \psi(\mathbf{r}_2) = 0. \tag{2.19}$$

The integrals are labeled as

$$A = \left\langle \phi(\mathbf{r}_1) \middle| \phi(\mathbf{r}_1) \right\rangle,$$
$$B = \left\langle \phi(\mathbf{r}_1) \middle| \frac{2}{\mathbf{r}_{12}} \phi(\mathbf{r}_1) \right\rangle,$$

and the symbol $\langle | \rangle$ denotes

$$\langle F | G \rangle = \int F(\mathbf{r}) G(\mathbf{r}) d^3 \mathbf{r}. \tag{2.20}$$

Hence, we obtain

$$\left[ \nabla_{\mathbf{r}_2}^2 - V^S(\mathbf{r}_2) + E_C \right] \psi(\mathbf{r}_2) = 0. \tag{2.21}$$

where the potential of the equation is

$$V^S(\mathbf{r_2}) = -\frac{2}{\mathbf{r}_2} + \frac{B}{A}. \tag{2.22}$$

22

Rewrite the potential as

$$V^S(r_2) = -\frac{2}{r_2} + \frac{B}{A} \tag{2.23}$$

since it only depends on the length of $r_1$ and not the position of the vector. The wave orbital
is

$$\psi(\mathbf{r}_2) = \frac{1}{r_2} \sum_{l=0}^{\infty} (2l+1) R_l(r_2) Y_{l,m}(\theta_2, \phi_2) \tag{2.24}$$

The spherical harmonics function is

$$Y_{l,m} = (-1)^m \sqrt{\frac{(2m+1)(l-m)}{(l+m)!}} P_{1,m}(cos\theta_2) e^{im\phi_2}. \tag{2.25}$$

We will be observing the ground state of hydrogen. In this case, the angular momentum
($l$) and azimuthal angle $m$ will be neglected for this orbital. This will yield just the radial
portion of the wave function. Now, let

$$R(r_2) = \frac{\psi(r_2)}{r_2}. \tag{2.26}$$

Hence, equation (2.21) becomes

$$\left[ \nabla_{r_2}^2 - V^S(r_2) + E_C \right] \psi(r_2) = 0. \tag{2.27}$$

This describes the position-hydrogen scattering equation.

### 2.3.2 Scattering Wave Equation for Electron-Hydrogen Scattering System

To determine the scattering wave function with exchange terms, utilize equation (2.9) and apply the following HFA

$$\Psi(\mathbf{r}_1, \mathbf{r}_2) = \sum_{i=1} \left[ \phi_i(\mathbf{r}_1)\psi_i(\mathbf{r}_2) \pm \phi_i(\mathbf{r}_2)\psi_i(\mathbf{r}_1) \right]. \tag{2.28}$$

When the $+$ sign is applied to the equation, the result will yield the triplet cases, and the $-$ sign yields the singlet cases. Then multiply by $\phi(\mathbf{r}_2)$, and integrate with respect to $\phi(\mathbf{r}_2)$. The following equation arises. Hence, equation (2.9) becomes

$$\int \phi(r_1) \left[ -\nabla^2_{\mathbf{r}_1} - \nabla^2_{\mathbf{r}_2} - \frac{2}{\mathbf{r}_1} - \frac{2}{\mathbf{r}_2} + \frac{2}{\mathbf{r}_{12}} - E \right] \left[ \phi_i(\mathbf{r}_1)\psi_i(\mathbf{r}_2) \pm \phi_i(\mathbf{r}_2)\psi_i(\mathbf{r}_1) \right] d^3\mathbf{r}_1 = 0. \tag{2.29}$$

Equation (2.29) can be written as

$$I_1 \pm I_2 = 0. \tag{2.30}$$

where

$$
\begin{aligned}
I_1 &= \int \phi(r_1) \left\{ -\nabla^2_{\mathbf{r}_1} - \nabla^2_{\mathbf{r}_2} - \frac{2}{\mathbf{r}_1} - \frac{2}{\mathbf{r}_2} + \frac{2}{\mathbf{r}_{12}} - E_C - E_B \right\} \phi(\mathbf{r}_1)\psi(\mathbf{r}_2) d^3\mathbf{r}_1 \\
&= \int \phi(\mathbf{r}_1) \left\{ -\nabla^2_{\mathbf{r}_2} - \frac{2}{\mathbf{r}_2} + \frac{2}{\mathbf{r}_{12}} - E_C \right\} \phi(\mathbf{r}_1)\psi(\mathbf{r}_2) d^3\mathbf{r}_1 \\
&\quad + \int \phi(\mathbf{r}_1) \left\{ -\nabla^2_{\mathbf{r}_1} - \frac{2}{\mathbf{r}_1} - E_B \right\} \phi(\mathbf{r}_1)\psi(\mathbf{r}_2) d^3\mathbf{r}_1
\end{aligned} \tag{2.31}
$$

and the weak asymptotic condition is applied. Then, we have

$$I_1 = \left\{ -\nabla^2_{\mathbf{r}_2} C - \frac{2}{\mathbf{r}_2}C + D - E_C C \right\} \psi(\mathbf{r}_2) \tag{2.32}$$

and

$$C = \Big\langle \phi(\mathbf{r}_1) \Big| \phi(\mathbf{r}_1) \Big\rangle,$$

$$D = \Big\langle \phi(\mathbf{r}_1) \Big| \frac{2}{\mathbf{r}_{12}} \phi(\mathbf{r}_1) \Big\rangle.$$

Now, we have

$$
\begin{aligned}
I_2 &= \int \phi(\mathbf{r}_1) \left\{ -\nabla_{\mathbf{r}_1}^2 - \nabla_{\mathbf{r}_2}^2 - \frac{2}{\mathbf{r}_1} - \frac{2}{\mathbf{r}_2} + \frac{2}{\mathbf{r}_{12}} - E_C - E_B \right\} \phi(\mathbf{r}_2)\psi(\mathbf{r}_1) d^3\mathbf{r}_1 \\
&= \int \phi(\mathbf{r}_1) \left\{ -\nabla_{\mathbf{r}_1}^2 - \frac{2}{\mathbf{r}_1} - E_B \right\} \phi(\mathbf{r}_2)\psi(\mathbf{r}_1) d^3\mathbf{r}_1 \\
&\quad + \int \phi(\mathbf{r}_1) \left\{ -\nabla_{\mathbf{r}_2}^2 - \frac{2}{\mathbf{r}_2} - E_B \right\} \phi(\mathbf{r}_2)\psi(\mathbf{r}_1) d^3\mathbf{r}_1 \\
&\quad + \int \phi(\mathbf{r}_1) \left\{ \frac{2}{\mathbf{r}_{12}} \right\} \phi(\mathbf{r}_2)\psi(\mathbf{r}_1) d^3\mathbf{r}_1 \\
&\quad + \int \phi(\mathbf{r}_1) \left\{ E_B - E_C \right\} \phi(\mathbf{r}_2)\psi(\mathbf{r}_1) d^3\mathbf{r}_1 \\
&= \left\{ \Big\langle \phi(\mathbf{r}_1) \frac{2}{\mathbf{r}_{12}} \psi(\mathbf{r}_1) \Big\rangle + (E_B - E_C) \Big\langle \phi(\mathbf{r}_1) | \psi(\mathbf{r}_1) \Big\rangle \right\} \phi(\mathbf{r}_2) \qquad (2.33)
\end{aligned}
$$

$$I_2 = \left\{ (E_B - E_C)E + F \right\} \phi(\mathbf{r}_2) \qquad (2.34)$$

where

$$E = \Big\langle \phi(\mathbf{r}_1) \Big| \psi(\mathbf{r}_1) \Big\rangle,$$

$$F = \Big\langle \phi(\mathbf{r}_1) \Big| \frac{2}{\mathbf{r}_{12}} \psi(\mathbf{r}_1) \Big\rangle.$$

Hence, we obtain the scattering wave function

$$- \left[ \nabla_{\mathbf{r}_2}^2 - V_S(\mathbf{r}_2) + E_C \right] \psi(\mathbf{r}_2) = \pm \frac{1}{C} \left[ (E_B - E_C)E + F \right] \phi(\mathbf{r}_2). \qquad (2.35)$$

and the potential energy is

$$V_S(r_2) = -\frac{2}{r_2}C + \frac{D}{C}. \tag{2.36}$$

To determine the radial wave function $R_l(r_2)$, the Legendre polynomials are expressed as $P_l(\cos\theta_2)$, and $l$ is the angular momentum. Apply (2.24) to (2.35), and then multiply by $P_l(\cos\theta_2)$ and integrated over the solid angle $d\Omega_1$ and let $l = 0$. The desired radial equation is obtained

$$-\left[\nabla_{r_2}^2 - V_S(r_2) + E_C\right]\psi(r_2) = \pm\frac{1}{C}\left[(E_B - E_C)E + F\right]\psi(r_2). \tag{2.37}$$

For simplicity, let $R_0(r_2) = \dfrac{\psi(r_2)}{r_2}$.

## 2.4    Schrödinger Equation for the Bound State Hydrogen Atom

We will also analyze the energy of the bound state electron. The general form of the radial equation is

$$\left[-\nabla_{r_1}^2 + \frac{l(l+1)}{r_1^2} + V(r_1)\right]\phi(r_1) = \varepsilon\phi(r_1), \tag{2.38}$$

where $\varepsilon = E_B$, the bound state energy. Chapter 5 will discuss how to find a similar equation for the bound state using the scattering state.

### 2.4.1    Summary of Governing Systems

In the section, we were able to arrive at the radial equations for the hydrogen atom, positron-hydrogen collision, and electron-hydrogen collision. We will proceed in the research with the following equations to determine the scattering and bound state approximate wave function for hydrogen,

$$\left[\nabla_{r_2}^2 - V^S(r_2) + E_C\right]\psi(r_2) = 0, \tag{2.39}$$

$$- \left[ \nabla_{r_2}^2 - V_S(r_2) + E_C \right] \psi = \pm \frac{1}{C} \left[ (E_B - E_C)E + F \right] \phi(r_2), \qquad (2.40)$$

and

$$\left[ - \nabla_{r_1}^2 + \frac{l(l+1)}{r_1^2} + V r_1 \right] \phi(r_1) = \varepsilon \phi(r_1). \qquad (2.41)$$

These equations will be applied to numerical methods to determine approximate solutions of the quantum states for hydrogen with the conditions stated in this chapter. Equation (2.39) is the equation governing the scattering state for positron-hydrogen collisions. Equation (2.40) is the equation governing the electron-hydrogen of collisions. Lastly, equation (2.41) is the equation governing the bound state of collisions.

# Chapter 3

# CALCULATION OF SCATTERING STATE USING NUMEROV METHOD

## 3.1 Overview

Numerov's method is used to solve second order differential equations without a first order term [66, 44]. The Numerov Algorithm yields sixth order accuracy. In quantum mechanics, this method is commonly used to solve for the wave function of scattering states. In this chapter, the general algorithm of Numerov's method is derived to solve a one-dimensional Schrödinger equation, and applied to positron-hydrogen and electron-hydrogen atomic collision to solve for the scattering state.

## 3.2 Derivation of the Numerov's Method

The Numerov's method is applied to second-order, linear, ordinary differential equations of the form

$$y''(x) + A(x)y(x) + B(x) = 0, \qquad y(a) = \alpha, \qquad y(b) = \beta. \tag{3.1}$$

The derivation of the Numerov algorithm is referenced from [66, 44]. Utilize the following Taylor series expansions with $y$ centered around $x + h$ and $x - h$:

$$y(x+h) = y(x) + y'(x)h + y''(x)\frac{h^2}{2!} + y'''(x)\frac{h^3}{3!} + y^{(4)}(x)\frac{h^4}{4!} + \dots \tag{3.2}$$

and

$$y(x-h) = y(x) - y'(x)h + y''(x)\frac{h^2}{2!} - y'''(x)\frac{h^3}{3!} + y^{(4)}(x)\frac{h^4}{4!} + \dots \tag{3.3}$$

28

The Taylor Expansions (3.2) and (3.3) are added together to get

$$y(x + h) - 2y(x) + y(x - h) = y''(x)\frac{h^2}{2} + y^{(4)}(x)\frac{h^4}{12} + O(h^6). \tag{3.4}$$

Solve for the second derivative

$$y''(x) = \frac{y(x + h) - 2y(x) + y(x - h)}{h^2} - y^{(4)}(x)\frac{h^2}{12} + O(h^6). \tag{3.5}$$

Then multiply (3.1) by $\left(1 + \frac{h^2}{12}\frac{d^2}{dx^2}\right)$

$$\frac{h^2}{12}y^{(4)}(x) + y''(x) + A(x)y(x) + B(x) + \frac{h^2}{12}\frac{d^2}{dx^2}[A(x)y(x) + B(x)] = 0. \tag{3.6}$$

Then replace the second derivative of (3.6) with (3.5).

$$\frac{h^2}{12}y^{(4)}(x) + \frac{y(x + h) - 2y(x) + y(x - h)}{h^2} - y^{(4)}(x) + A(x)y(x) + B(x)$$
$$+ \frac{h^2}{12}\frac{d^2}{dx^2}[A(x)y(x) + B(x)] = 0 \tag{3.7}$$

Using the second derivative approximation for $\frac{d^2}{dx^2}[A(x)y(x) + B(x)]$, we obtain

$$\frac{d^2}{dx^2}[A(x)y(x) + B(x)] \simeq \frac{A(x + h)y(x + h) - 2A(x)y(x) + A(x + h)y(x - h)}{h^2}$$
$$+ \frac{B(x + h) - 2B(x) + B(x - h)}{h^2}. \tag{3.8}$$

Apply this approximation to equation (3.7).

$$\frac{A(x+h)y(x+h) - 2A(x)y(x) + A(x+h)y(x-h)}{12} + \frac{B(x+h) - 2B(x) + B(x-h)}{12}$$
$$\frac{y(x+h) - 2y(x) + y(x-h)}{h^2} + A(x)y(x) + B(x) = 0. \tag{3.9}$$

Combine like terms

$$y(x+h)\left(\frac{1}{h^2} + \frac{A(x+h)}{12}\right) + y(x)\left(-\frac{2}{h^2} + \frac{10}{12}\right) + y(x-h)\left(\frac{1}{h^2} + \frac{A(x+h)}{12}\right)$$
$$+ \frac{B(x+h) + 10B(x) + B(x-h)}{12} = 0. \tag{3.10}$$

Finally, solve for $y(x+h)$, and the algorithm for a non-homogeneous ordinary differential is as follows:

$$y_{n+1} = \frac{(2 - \frac{10h^2}{12}A_n)y_n - (1 + \frac{h^2}{12}A_{n-1})y_{n-1} + \frac{h^2}{12}\left(B_{n+1} + \frac{10}{12}B_n(x) + B_{n-1}\right)}{1 + \frac{h^2}{12}A_{n+1}}. \tag{3.11}$$

## 3.3    Application to Positron and Electron Hydrogen Collisions

Recall the Schrödinger equations for positron-hydrogen (2.39) and electron-hydrogen (2.40) collisions in Chapter 2. Numerov's algorithm can be easily applied to those problems by letting $A(x) = E_C - V_S$. In the positron-hydrogen case, $B(x) = 0$. For electron hydrogen, the exchange terms are present and $B(x) = \{(E_B - E_C)C + D\}\phi$.

The known behavior of the scattering wave function is of the form $\sin(kr_m + \delta)$. To determine the accuracy of the computed approximation, the solution is plotted to insure it has the sine wave behavior and the phase shift denoted by $\delta$, is found for the corresponding

incident energy, $E_C = k^2$. The $\delta$ is calculated by the Sum and Difference Identities.

$$\psi(r_m) = \sin(kr_m + \delta) \tag{3.12}$$

$$= A\sin(kr_m) + B\cos(kr_m) \tag{3.13}$$

where

$$A = \cos(\delta), \tag{3.14}$$

$$B = \sin(\delta). \tag{3.15}$$

Then take the derivative of $\psi$ and form a linear system.

$$\psi'(r_m) = kA\cos(kr_m) - kB\sin(kr_m) \tag{3.16}$$

$$\begin{pmatrix} \psi(r_m) \\ \psi'(r_m) \end{pmatrix} = \begin{pmatrix} \sin(kr_m) & \cos(kr_m) \\ k\cos(kr_m) & -k\sin(kr_m) \end{pmatrix} \begin{pmatrix} A \\ B \end{pmatrix}. \tag{3.17}$$

Solve for A and B.

$$A = \frac{k\sin(kr_m)\psi(r_m) + \cos(kr_m)\psi'(r_m)}{k}, \tag{3.18}$$

$$B = \frac{k\cos(kr_m)\psi(r_m) - \sin(kr_m)\psi'(r_m)}{k}, \tag{3.19}$$

$$\delta = \arctan(B/A). \tag{3.20}$$

Finally, $\delta$ is determined by taking the arc tangent of $\dfrac{B}{A}$.

### 3.3.1 Application of Numerov's Method and Numerical Results

Numerov's method is utilized to determine the phase shift and profile of the scattering function for (2.39) and (2.40). In most numerical algorithms, the reduction of the spatial or time step results in reduced error of the approximation, which is desirable for numerical calculations. Numerov method has a unique disadvantage in that reduction of the spatial step, $h$, causes the influence of $B(x)$ in the algorithm to become smaller, which can be undesirable. Hence, caution must be taken in choosing appropriate value of $h$ in computation. Results are emphasized in bold that are the same as the analytic solutions from John [34].

### 3.3.1.1 Numerical Results without Exchange Terms

For the positron-hydrogen case, Numerov's method was applied without exchange terms to the scattering state at low energies. These results were achieved with spaital step of $h = 0.01$. When comparing our results with other variational methods, we have obtained acceptable results. For continuum energies $0.06 \leq E_C \leq 0.4$, the phase shifts computed in this dissertation where the same those found in [34].

**Table 3.1:** The phase shifts, $\delta$, for the continuum function without exchange and their corresponding energies. The numerical results from [34] are compared with the approximate phase shifts found using Numerov.

| $k^2$ | Variational Method $\delta$ | Numerov Method $\delta$ |
|---|---|---|
| 1.0 | 0.9055 | 0.9045 |
| 0.8 | 0.9356 | 0.9347 |
| 0.5 | 0.9909 | 0.9901 |
| 0.4 | 1.012 | **1.012** |
| 0.3 | 1.034 | **1.034** |
| 0.25 | 1.045 | **1.044** |
| 0.2 | 1.053 | **1.053** |
| 0.15 | 1.058 | **1.057** |
| 0.1 | 1.050 | **1.050** |
| 0.08 | 1.039 | **1.039** |
| 0.06 | 1.017 | **1.017** |
| 0.05 | 0.9991 | 0.9987 |
| 0.04 | 0.9726 | 0.9722 |
| 0.03 | 0.9317 | 0.9312 |
| 0.02 | 0.8626 | 0.8621 |
| 0.015 | 0.8070 | 0.8064 |
| 0.01 | 0.5727 | 0.5728 |

### 3.3.1.2   Numerical Results with Exchange Terms

When computing the electron-hydrogen case, there where some difficulties with convergence for the singlet case for continuum energies $0.03 \leq E_C \leq 1.0$. Table 3.2 shows that most energies diverged except the continuum energies $0.01 \leq E_C \leq 0.02$. In order to reach convergence with a relative error of order 6, at at least 50 iterations were required.

The triplet case was convergent for all low energies ($0.01 \leq E_C \leq 1.0$). The phase shifts obtained were exactly the same as those found in [34]. We were able to achieve convergence with 30 iterations or less. The results for the triplet case can be found in Table 3.3.

**Table 3.2:** The phase shifts, $\delta$, for the continuum function with exchange terms of the singlet case and their corresponding energies. The numerical solutions from [34] are used to compare with the approximate phase shifts found using Numerov.

| $k^2$ | Variational Method $\delta$ | Numerov Method $\delta$ |
|---|---|---|
| 0.02 | 2.153 | 2.149 |
| 0.015 | 2.259 | 2.239 |
| 0.01 | 2.396 | 2.397 |

**Table 3.3:** The phase shifts, $\delta$, for the continuum function with exchange terms of the triplet case and their corresponding energies. The numerical solutions from [34] are used to compare with the approximate phase shifts found using Numerov.

| $k^2$ | Variational Method $\delta$ | Numerov Method $\delta$ |
|---|---|---|
| 1.0 | 1.391 | **1.391** |
| 0.8 | 1.501 | **1.501** |
| 0.5 | 1.739 | **1.739** |
| 0.4 | 1.849 | **1.849** |
| 0.3 | 1.987 | **1.987** |
| 0.25 | 2.070 | **2.070** |
| 0.2 | 2.167 | **2.167** |
| 0.15 | 2.282 | **2.282** |
| 0.1 | 2.427 | **2.427** |
| 0.08 | 2.498 | **2.498** |
| 0.06 | 2.580 | **2.580** |
| 0.05 | 2.627 | **2.627** |
| 0.04 | 2.679 | **2.679** |
| 0.03 | 2.739 | 2.740 |
| 0.02 | 2.812 | 2.812 |
| 0.015 | 2.856 | 2.857 |
| 0.01 | 2.908 | 2.929 |

# Chapter 4

# GREEN'S FUNCTION METHODS TO CALCULATE THE SCATTERING WAVE FUNCTION OF ELECTRON-HYDROGEN

## 4.1 Overview

In this chapter, an innovative numerical method is explored using the Green's function of the Schrödinger equation governing electron-hydrogen scattering. The development of the method by Zerrad [69] to use the singular value decomposition (SVD) to address the non-local kernel is discussed as well as the improvements made to achieve more accurate results for the hydrogen atom.

## 4.2 Green's Function Method

The method described here consists of taking the non-local kernel into account perturbatively; however, as shown the method fails when the successive iterations diverge when simple algorithms are applied. The procedure consists in writing equation (2.40) in the form

$$\left[ \frac{d^2}{dr_2^2} - V(r_2) + E_C \right] R_o(r_2) = \pm \int_0^\infty \mathcal{F}(r_1, r_2) R_o(r_1) dr_1, \qquad (4.1)$$

and then transforming it into the iterative integral equation

$$R_0^{(n+1)}(r_2) = f(r_2) + \int_0^\infty G_V(r_2, \xi) \left( \pm \int_0^\infty \mathcal{F}(\xi, r_1) R_0^{(n)}(r_1) dr_1 \right) d\xi. \qquad (4.2)$$

In the above, $f(r_2)$ is the homogeneous solution of

$$\left[ \frac{d^2}{dr_2^2} - V(r_2) + E_C \right] f(r_2) = 0, \qquad (4.3)$$

and $G_V(r_2, \xi)$ is the Green's function which corresponds to the left-hand-side of equation (4.1). It is distorted by the local $V$, and can be expressed in terms of semi-separable expressions involving two independent solutions $f(x_2)$ and $g(x_2)$ of equation (4.3),

$$G_V(r_2, \xi) = \frac{1}{W(r_2, \xi)} f(r_2) g(\xi) \qquad r_2 \leq \xi, \tag{4.4}$$

$$G_V(r_2, \xi) = \frac{1}{W(r_2, \xi)} f(\xi) g(r_2) \qquad r_2 > \xi. \tag{4.5}$$

The Wronskian $W(r_2, \xi)$ is

$$W(r_2, \xi) = \frac{1}{f(r_2) g'(\xi) - g(r_2) f'(\xi)} \tag{4.6}$$

The iteration is started by using the solution in the absence of the exchange terms for the first $(n = 0)$ guess: $R_o^{(0)} = f(r_2)$.

The rate of convergence of the iterations depends on the norm of

$$F_V(r_2, z) = \int_0^\infty G_V(r_2, \xi) \mathcal{F}(\xi, z) \, d\xi. \tag{4.7}$$

This norm in turn depends on the norm of $\mathcal{F}$, and the norm of $G_V$. The latter becomes large at small incident energies $k^2$, in view of the overt presence of the factor $1/k$ in equation (4.5). The convergence also depends on the $\pm$ sign in front of the exchange integrals. This can be seen by writing the iterative series as

$$R_0^{(n+1)} = [1 + (\pm F_V) + (\pm F_V)^2 + (\pm F_V)^3 + \ldots (\pm F_V)^n], \tag{4.8}$$

which for large values of $n$ is symbolically of the form $[1 \pm F_V]^{-1}$, and hence may converge

or diverge in the vicinity of the point "one" according to whether the effective sign of the operator $\pm F_V$ is positive or negative.

### 4.2.1 Numerical iteration of the Schrödinger Equation using the SVD Method to Separate the Non-local Kernel

In what follows in this section, we describe a method which reduces the norm of the non-local kernel $\mathcal{F}$ by decomposing it into a number of fully separable kernels plus a remainder. The separable terms are placed on the left hand side of equation (4.1), the Green's function in the presence of both the local distorting potential $V$ and the separable non-local pieces of the kernel is obtained, and hence iterations of the form of equation (4.2) can be carried out, where $\mathcal{F}$ is not the residual kernel. This way, the divergence can be shifted to smaller values $k$, but it cannot be avoided.

The SVD is utilized to decompose the kernel $\mathcal{F}(r_1, r_2)$ into a number of fully separable terms plus a remainder. A brief description of the method follows.

A numerical integration algorithm is chosen which divides the range of integration $[0, \mathrm{R_{max}}]$ into a set of $N$ discrete points. Correspondingly, the kernel $\mathcal{F}(r_1, r_2)$ is transformed into a $N \times N$ matrix $K(i, j)$, with $i = 1, 2, \ldots N$, and likewise for $j$. We perform a singular value decomposition on $K$. The SVD method is based on the following theorem of linear algebra [31]: Any $M \times N$ matrix $K$ whose number of rows $M$ is greater than or equal to its number of columns $N$, can be written as the product of an $M \times N$ matrix, $U$, an $N \times N$ diagonal matrix, $\sigma$, with non-negative elements, and the transpose of an $N \times N$ matrix, $V$. The column vectors of $U$ are the orthonormal eigenvectors of the matrix $KK^\top$ and the column vectors of $V$ are the orthonormal eigenvectors of the matrix $K^\top K$. $\sigma$ contains the square roots of the singular values (eigenvalues of $KK^\top$ ordered from greatest to

smallest along the diagonal. Thus,

$$\sum_{i=1}^{M} u_{is}u_{ir} \;=\; \delta_{sr} \qquad 1 \le s, r \le N, \tag{4.9}$$

$$\sum_{i=1}^{M} v_{si}v_{ri} \;=\; \delta_{sr} \qquad 1 \le s, r \le N. \tag{4.10}$$

Hence, we can write the matrix $K$ as

$$K = U\sigma V^{\top} \tag{4.11}$$

with matrix elements

$$K(i,j) = \sum_{s=1}^{N} u_{is}\sigma_s v_{sj}^{\top} \tag{4.12}$$

As a result, a fully separable piece of rank $n$ can be separated out of the matrix $K$, leaving a residual matrix, $K_r$,

$$K(i,j) = K_s(i,j) + K_r(i,j). \tag{4.13}$$

Computing the sum in equation (4.12) to an upper limit $n$ which includes only the $n$ largest values $\sigma_s$, we obtain

$$K_s(i,j) = \sum_{s=1}^{n} u_{is}\sigma_s v_{sj}^{\top}. \tag{4.14}$$

and the remainder

$$K_r(i,j) = K(i,j) - K_s(i,j) = \sum_{s=n+1}^{N} u_{is}\sigma_s v_{sj}^{\top}. \tag{4.15}$$

We utilize the SVD of $K$ in equation (4.1) where $\mathcal{F}(r_1, r_2)$ is computed as $K$. Hence for

$K = K_s + K_r$ we obtain,

$$\psi'' + (E_c - V)\psi \;=\; \int (K_s + K_r)\psi, \tag{4.16}$$

$$\psi'' + (E_c - V)\psi - \int K_s\psi \;=\; \int K_r\psi. \tag{4.17}$$

The homogeneous solution of equation (4.17) is the solution of

$$\psi'' + (E_c - V)\psi = \int K_s\psi \tag{4.18}$$

which is denoted by $\psi_h$ where

$$\psi_h = f + \int G_V \int K_s\psi_h. \tag{4.19}$$

Hence, we get

$$\psi \;=\; \psi_h + \int G_{V+K_s} \int K_r\psi \tag{4.20}$$

$$\psi \;=\; f + \int G_V \int K_s\psi + \int G_{V+K_s} \int K_r\psi \tag{4.21}$$

$$\tag{4.22}$$

where

$$\psi = \int G_{V+K_s} \int K_r\psi \tag{4.23}$$

is the non-homogeneous solution to equation (4.17).

Now assume

$$\psi = f + \int G_V \int K_s\psi + G_V \int K_r\psi \tag{4.24}$$

Dropping the integral signs, we get

$$\psi = f + G_V K_s \psi + G_V K_r \psi, \tag{4.25}$$

$$\psi = f + G_V u \sigma \left[ v^\top \psi \right] + G_V K_r \psi. \tag{4.26}$$

Multiplying equation (4.26) by $\sqrt{\sigma} v^\top$ and integrating, we obtain

$$\sqrt{\sigma} v^\top \psi = \sqrt{\sigma} v^\top f + \sqrt{\sigma} v^\top G_V u \sigma \left[ v^\top \psi \right] + \sqrt{\sigma} v^\top G_V K_r \psi \tag{4.27}$$

$$\sqrt{\sigma} v^\top \psi = \sqrt{\sigma} v^\top f + \sqrt{\sigma} v^\top G_V u \sigma v^\top \psi + \sqrt{\sigma} v^\top G_V K_r \psi \tag{4.28}$$

$$\sqrt{\sigma} v^\top \psi - \sqrt{\sigma} v^\top G_V u \sigma v^\top \psi = \sqrt{\sigma} v^\top f + \sqrt{\sigma} v^\top G_V K_r \psi \tag{4.29}$$

$$\left( I - \sqrt{\sigma} v^\top G_V u \sqrt{\sigma} \right) \sqrt{\sigma} v^\top \psi = \sqrt{\sigma} v^\top f + \sqrt{\sigma} v^\top G_V K_r \psi \tag{4.30}$$

$$M \sqrt{\sigma} v^\top \psi = \sqrt{\sigma} v^\top f + \sqrt{\sigma} v^\top G_V K_r \psi \tag{4.31}$$

where

$$M = I - \sqrt{\sigma} v^\top G_V u \sqrt{\sigma}. \tag{4.32}$$

This leads to

$$v^\top \psi = \sqrt{\sigma}^{-1} M^{-1} \left( \sqrt{\sigma} v^\top f + \sqrt{\sigma} v^\top G_V K_r \psi \right) \tag{4.33}$$

$$\left[ v^\top \psi \right] = \sqrt{\sigma}^{-1} M^{-1} \sqrt{\sigma} v^\top \left( f + G_V K_r \psi \right) \tag{4.34}$$

Now, substitute the expression for $\left[v^\top \psi\right]$ from equation (4.34) into equation (4.26) to obtain

$$
\begin{align}
\psi &= f + G_V u\sqrt{\sigma} M^{-1} \sqrt{\sigma} v^\top (f + K_r \psi) + G_V K_r \psi \tag{4.35}\\
\psi &= \left(I + G_V u\sqrt{\sigma} M^{-1} \sqrt{\sigma} v^\top\right)(f + G_V K_r \psi) \tag{4.36}
\end{align}
$$

Hence, the non-homogeneous solution of equation (4.17) can be written as

$$
\psi = \int G_{V+K_s} \left( f + \int G_V \int K_r \psi \right) \tag{4.37}
$$

where

$$
G_{V+K_s} = I + G_V u\sqrt{\sigma} M^{-1} \sqrt{\sigma} v^\top. \tag{4.38}
$$

In order to obtain the Green's function, $G_{V+K^S}(x, \xi)$, which is distorted by both the local potential $V$ and the fully separable kernel $K^S$, we rewrite equation (4.2) symbolically in the form

$$
\psi'' + (E_C - V)\psi = \int (K_s + K_r)\psi \tag{4.39}
$$

$$
\mathcal{L}\psi = \int (K_s + K_r)\psi \tag{4.40}
$$

$$
\mathcal{L}\psi = 0 \tag{4.41}
$$

$$
\mathcal{L}\psi = \int K_s \psi \tag{4.42}
$$

$$
\psi'' + (k^2 - V)\psi - \int K_s \psi = \int K_r \psi \tag{4.43}
$$

$$
\bar{\mathcal{L}}\psi = \int K_r \psi. \tag{4.44}
$$

41

## 4.3   Numerical Results

As expected, using the Green's Function Method without separating the non-local kernel was divergent for most low energies. Tables 4.1 and 4.2 show the continuum energies that were convergent for the singlet and triplet cases.

Tables 4.3 and 4.4 contains phase shifts that utilize the SVD method to separate the kernel for all low energies for the continuum state. The convergence was achieved in less than 5 iterations with sixth order accuracy. Comparing our results to those found in [34], for the triplet case, we were able to get the exact values. The range $0.04 \leq E_C \leq 1$ produced the exact same phase shifts. For the singlet case, the phase shifts found are acceptable. The phase shifts are accurate to 3 decimal places.

Tables 4.5 and 4.6 compare all numerical methods used to solve the electron-hydrogen scattering phase shifts. It is clear that the SVD method performs better than Numerov and the Green's function for the triplet and singlet cases.

**Table 4.1:** The phase shifts, $\delta$, for the continuum function with exchange terms for the singlet case and their corresponding energies. The numerical solutions from [34] are used to compare with the approximate phase shifts found using the Green's function.

| $E_C$ | Variational Method | Green's Function Method |
|-------|--------------------|--------------------------|
| 1.0   | 0.5429             | 0.5428                   |
| 0.8   | 0.5888             | 0.5887                   |
| 0.2   | 1.135              | 1.135                    |
| 0.15  | 1.270              | 1.270                    |
| 0.1   | 1.460              | 1.459                    |
| 0.08  | 1.563              | 1.560                    |

**Table 4.2:** The phase shifts, $\delta$, for the continuum function with exchange terms for the triplet case and their corresponding energies. The numerical solutions from [34] are used to compare with the approximate phase shifts found using the Green's function.

| $E_C$ | Variational Method | Green's Function Method |
|---|---|---|
| 1.0 | 1.391 | 1.390 |
| 0.8 | 1.501 | 1.500 |
| 0.25 | 2.070 | 2.068 |
| 0.2 | 2.167 | 2.162 |
| 0.15 | 2.282 | 2.281 |
| 0.1 | 2.427 | 2.427 |
| 0.08 | 2.498 | 2.477 |

**Table 4.3:** The phase shifts, $\delta$, for the continuum function with exchange terms for the singlet case and their corresponding energies. The numerical solutions from [34] are used to compare with the approximate phase shifts found using SVD.

| $E_C$ | Variational Method | SVD Method |
|---|---|---|
| 1.0 | 0.5429 | 0.5428 |
| 0.8 | 0.5888 | 0.5887 |
| 0.5 | 0.7370 | 0.7365 |
| 0.4 | 0.8248 | 0.8247 |
| 0.3 | 0.9488 | 0.9489 |
| 0.25 | 1.031 | 1.032 |
| 0.2 | 1.135 | 1.135 |
| 0.15 | 1.270 | 1.270 |
| 0.1 | 1.460 | 1.459 |
| 0.08 | 1.563 | 1.562 |
| 0.06 | 1.693 | 1.692 |
| 0.05 | 1.774 | 1.773 |
| 0.04 | 1.871 | 1.870 |
| 0.03 | 1.992 | 1.990 |
| 0.02 | 2.153 | 2.152 |
| 0.015 | 2.259 | 2.238 |
| 0.01 | 2.396 | 2.396 |

**Table 4.4:** The phase shifts, $\delta$, for the continuum function with exchange terms for the triplet case and their corresponding energies. The numerical solutions from [34] are used to compare with the approximate phase shifts found using SVD.

| $E_C$ | Variational Method | SVD Method |
|---|---|---|
| 1.0 | 1.391 | **1.391** |
| 0.8 | 1.501 | **1.501** |
| 0.5 | 1.739 | **1.739** |
| 0.4 | 1.849 | **1.849** |
| 0.3 | 1.987 | **1.987** |
| 0.25 | 2.070 | **2.070** |
| 0.2 | 2.167 | **2.167** |
| 0.15 | 2.282 | **2.282** |
| 0.1 | 2.427 | **2.427** |
| 0.08 | 2.498 | **2.498** |
| 0.06 | 2.580 | **2.580** |
| 0.05 | 2.627 | **2.627** |
| 0.04 | 2.679 | **2.679** |
| 0.03 | 2.739 | 2.740 |
| 0.02 | 2.812 | 2.812 |
| 0.015 | 2.856 | 2.861 |
| 0.01 | 2.908 | 2.929 |

**Table 4.5:** The phase shifts, $\delta$, for the continuum function with exchange terms for the singlet case and their corresponding energies. The analytic solutions from [34] are used to compare with the approximate phase shifts found using all numerical techniques in Chapter 3 and this chapter. Note: - - Indicates that convergence was not achieved at this energy.

| $E_C$ | Variational Method | Numerov Method | Green's Function Method | SVD Method |
|---|---|---|---|---|
| 1.0 | 0.5429 | - - | 0.5428 | 0.5428 |
| 0.8 | 0.5888 | - - | **0.5888** | 0.5887 |
| 0.5 | 0.7370 | - - | - - | 0.7365 |
| 0.4 | 0.8248 | - - | - - | 0.8247 |
| 0.3 | 0.9488 | - - | - - | 0.9489 |
| 0.25 | 1.031 | - - | - - | 1.032 |
| 0.2 | 1.135 | - - | **1.135** | **1.135** |
| 0.15 | 1.270 | - - | **1.270** | **1.270** |
| 0.1 | 1.460 | - - | 1.459 | 1.459 |
| 0.08 | 1.563 | - - | 1.560 | 1.562 |
| 0.06 | 1.693 | - - | - - | 1.692 |
| 0.05 | 1.774 | - - | - - | 1.773 |
| 0.04 | 1.871 | - - | - - | 1.870 |
| 0.03 | 1.992 | - - | - - | 1.990 |
| 0.02 | 2.153 | 2.149 | - - | 2.152 |
| 0.015 | 2.259 | **2.259** | - - | **2.259** |
| 0.01 | 2.396 | 2.397 | - - | **2.396** |

**Table 4.6:** The phase shifts, $\delta$, for the continuum function with exchange terms for the triplet case and their corresponding energies. The analytic solutions from [34] are used to compare with the approximate phase shifts found using all numerical techniques in Chapter 3 and this chapter. Note: - - Indicates that convergence was not achieved at this energy.

| $E_C$ | Variational Method | Numerov Method | Green's Function Method | SVD Method |
|-------|-------------------|----------------|------------------------|------------|
| 1.0 | 1.391 | **1.391** | 1.390 | **1.391** |
| 0.8 | 1.501 | **1.501** | 1.500 | **1.501** |
| 0.5 | 1.739 | **1.739** | - - | **1.739** |
| 0.4 | 1.849 | **1.849** | - - | **1.849** |
| 0.3 | 1.987 | **1.987** | - - | **1.987** |
| 0.25 | 2.070 | **2.070** | 2.068 | **2.070** |
| 0.2 | 2.167 | **2.167** | 2.162 | **2.167** |
| 0.15 | 2.282 | **2.282** | 2.281 | **2.282** |
| 0.1 | 2.427 | **2.427** | **2.427** | **2.427** |
| 0.08 | 2.498 | **2.498** | 2.477 | **2.498** |
| 0.06 | 2.580 | **2.580** | - - | **2.580** |
| 0.05 | 2.627 | **2.627** | - - | **2.627** |
| 0.04 | 2.679 | **2.679** | - - | **2.679** |
| 0.03 | 2.739 | 2.740 | - - | 2.740 |
| 0.02 | 2.812 | **2.812** | - - | **2.812** |
| 0.015 | 2.856 | 2.857 | - - | 2.861 |
| 0.01 | 2.908 | 2.929 | - - | 2.929 |

# Chapter 5

# ENERGY MATCHING METHOD TO SOLVE THE BOUND STATE WAVE FUNCTION

## 5.1 Overview

In this chapter, an energy matching method will be implemented to determine energy eigenvalues and their eigenfuntions. This method will be used to solve bound state electrons. The radial Schrödinger equation for a static hydrogen atom will be used to illustrate this numerical method.

## 5.1.1 Derivation of Energy Matching Method for the Hydrogen Atom

We reference the stationary radial hydrogen atom equation that was mentioned in Chapter 2.

$$\left[ \frac{d^2}{dr^2} - \frac{l(l+1)}{r^2} - V(r) + \varepsilon \right] \phi(r) = 0. \tag{5.1}$$

The boundary conditions are

$$\phi(0) \quad = \quad 0, \tag{5.2}$$

$$\phi \quad \rightarrow \quad 0 \quad \text{as} \quad r \rightarrow \infty. \tag{5.3}$$

The normality condition is

$$\int_0^\infty \phi^*(r')\phi(r')dr' = 1. \tag{5.4}$$

Since the equation is homogeneous, the solution can be determined by solving (5.1) with the boundary conditions and then normalizing the solution. Equation (5.1) contains a parameter $\varepsilon$ that must be found to satisfy the boundary conditions. This parameter can be

found by integrating out with the left boundary condition and integrating in with the right boundary condition. We adjust the energy, $\varepsilon$, until the solutions meet at some intermediate radius. The solutions to the outward and inward integration are arbitrary to the extent of a multiplicative constant. The solution of the outward integration will be labeled $\phi_{out}$, and the solution of the inward integration is labeled $\phi_{in}$. The outward and inward solutions are matched at a radius $r_0$ and the matching condition is

$$\frac{\frac{d}{dr}[\phi_{out}(r_0)]}{\phi_{out}(r_0)} = \frac{\frac{d}{dr}[\phi_{in}(r_0)]}{\phi_{in}(r_0)}. \tag{5.5}$$

The multiplicative constants of the inward and outward solutions are chosen so that the coordinates $\phi(r_0)_{out}$ and $\phi(r_0)_{in}$ of the graphs of the solution at $r = r_0$ are equal and the slopes of the curves of these solutions at $r_0$ equal also.

The integration of the first trial value of $\varepsilon$ will probably not match at $r = r_0$. An estimate of $\Delta\varepsilon$ that produces a match can be obtained from the degree of mismatch, as measured by the difference between the values of $\frac{\frac{d}{dr}[\phi_{out}(r_0)]}{\phi_{out}(r_0)}$ and $\frac{\frac{d}{dr}[\phi_{in}(r_0)]}{\phi_{in}(r_0)}$. Let $\phi + \Delta\phi$ be the solution of equation (5.1) and let $\varepsilon$ be replaced by $\varepsilon + \Delta\varepsilon$. Hence,

$$\left[\frac{d^2}{dr^2} - V(r) + (\varepsilon + \Delta\varepsilon)\right](\phi + \Delta\phi) = 0. \tag{5.6}$$

Then

$$\left[\frac{d^2}{dr^2} - V(r) + (\varepsilon + \Delta\varepsilon)\right]\Delta\phi = -\phi\Delta\varepsilon. \tag{5.7}$$

We restrict the equation to contain only first-order terms. The second-order terms are

neglected. Now the equation can be written as

$$\left[\frac{d^2}{dr^2} - V(r) + \varepsilon\right]\Delta\phi = -\phi\Delta\varepsilon. \tag{5.8}$$

Multiply (5.6) by $\phi$ and (5.7) by $-\Delta\phi$ and add them together. This gives

$$\phi(r)\frac{d^2}{dr^2}\Delta\phi(r) - \Delta\phi(r)\frac{d^2}{dr^2}\phi(r) = -\phi(r)^2\Delta\varepsilon. \tag{5.9}$$

The left hand side is $\dfrac{d}{dr}[\phi(r)\Delta\phi'(r) - \phi'(r)\Delta\phi(r)]$ since $\Delta\phi$ is the difference between the values of the two solutions at the same value of r. Thus, integration of equation (5.9) gives

$$\phi(r)\Delta\phi'(r) - \phi'(r)\Delta\phi(r)|_a^b = -\Delta\varepsilon\int_a^b\phi(r)^2dr'. \tag{5.10}$$

For the outward integration, $\phi = \Delta\phi = 0$ at $r = 0$ taken at $r = r_0$

$$(\phi(r_0)\Delta\phi(r_0)' - \phi'(r_0)\Delta\phi(r_0))_{out} = -\Delta\varepsilon\int_0^{r_0}\phi(r_0)^2dr'. \tag{5.11}$$

Next, for the inward integration $\phi = \Delta\phi = 0$ at $r = \infty$ taken at $r = r_0$

$$-(\phi(r_0)\Delta\phi'(r_0) - \phi'(r_0)\Delta\phi(r_0))_{in} = -\Delta\varepsilon\int_{r_0}^{\infty}\phi(r_0)^2dr'. \tag{5.12}$$

Let $\Delta\left(\dfrac{\phi(r_0)'}{\phi(r_0)}\right) = \dfrac{\phi\Delta\phi' - \phi'\Delta\phi}{\phi^2}$ so that

$$\Delta\left(\frac{\phi(r_0)'}{\phi(r_0)}\right)_{out} = -\Delta\varepsilon\frac{\int_0^{r_0}\phi(r_0)_{out}^2dr'}{\phi(r_0)_{out}^2}, \tag{5.13}$$

49

$$\Delta \left( \frac{\phi(r_0)'}{\phi(r_0)} \right)_{in} = \Delta \varepsilon \frac{\int_{r_0}^{\infty} \phi(r_0)_{in}^2 dr'}{\phi(r_0)_{in}^2}. \tag{5.14}$$

If the inward integration and outward integration have been carried out for some trial value $\varepsilon$ and give values for $\left( \frac{\phi'}{\phi} \right)_{out}$ and $\left( \frac{\phi'}{\phi} \right)_{in}$ that do not match, we change $\Delta \varepsilon$ of $\varepsilon$ such that

$$\left( \frac{\phi'}{\phi} \right)_{out} + \Delta \left( \frac{\phi'}{\phi} \right)_{out} = \left( \frac{\phi'}{\phi} \right)_{in} + \Delta \left( \frac{\phi'}{\phi} \right)_{in}. \tag{5.15}$$

Utilizing (5.13) and (5.14), the required change of $\varepsilon$ is

$$- \left[ \frac{\int_{r_0}^{\infty} \phi(r_0)_{in}^2 dr'}{\phi(r_0)_{in}^2} + \frac{\int_0^{r_0} \phi(r_0)_{out}^2 dr'}{\phi(r_0)_{out}^2} \right] \Delta \varepsilon = \left[ \left( \frac{\phi(r_0)'}{\phi(r_0)} \right)_{out} - \left( \frac{\phi(r_0)'}{\phi(r_0)} \right)_{in} \right]. \tag{5.16}$$

Then we have

$$\Delta \varepsilon = \frac{\left[ \left( \frac{\phi(r_0)'}{\phi(r_0)} \right)_{in} - \left( \frac{\phi(r_0)'}{\phi(r_0)} \right)_{out} \right]}{\left[ \frac{\int_{r_0}^{\infty} \phi(r_0)_{in}^2 dr'}{\phi(r_0)_{in}^2} + \frac{\int_0^{r_0} \phi(r_0)_{out}^2 dr'}{\phi(r_0)_{out}^2} \right]}. \tag{5.17}$$

## 5.2   Numerical Results

The energy matching method was utilized to solve energy eigenvalues for the bound state hydrogen for $n = 4$ quantum states. The ground state ($1s$) orbital energy and the excited states ($2s, 3s, 4s$) where computed with accuracy of order 3. The exact eigenvalues for the hydrogen atom are of the form $1/n^2$ where $n$ is the principal quantum number that describes the size of the orbital. Figures 5.1, 5.2, 5.3 and 5.4, show the eigenfunctions and their corresponding eigenvalues found using the energy matching method.

Table 5.1 shows how choosing the match ($r_0$) has significant effect on the eigenvalue energies and eigenfunctions. As the match was increased, the solutions were inaccurate for guesses ($E_{B_0}$) that were in the $3s$ and $4s$ energy range. When applying this numerical

method, the solution was very sensitive when changing the spatial step. Changing the spatial step required a change in the match, as well. This phenomenon was discovered when attempting convergence for higher orbitals.
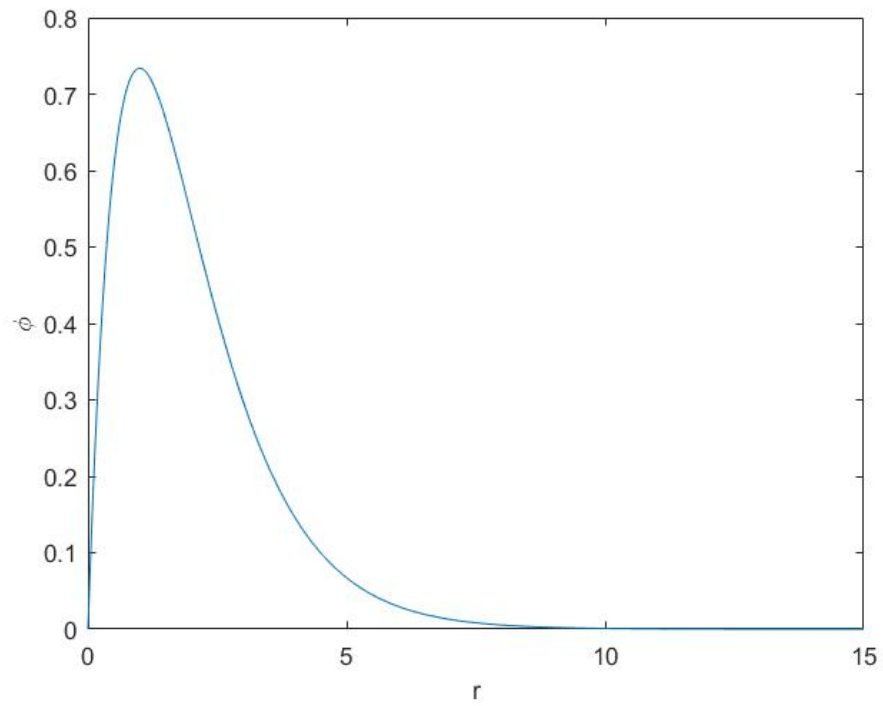
**Figure 5.1:** Eigenfunction for the 1s orbital and its corresponding energy eigenvalue with $\varepsilon = -0.9984$.
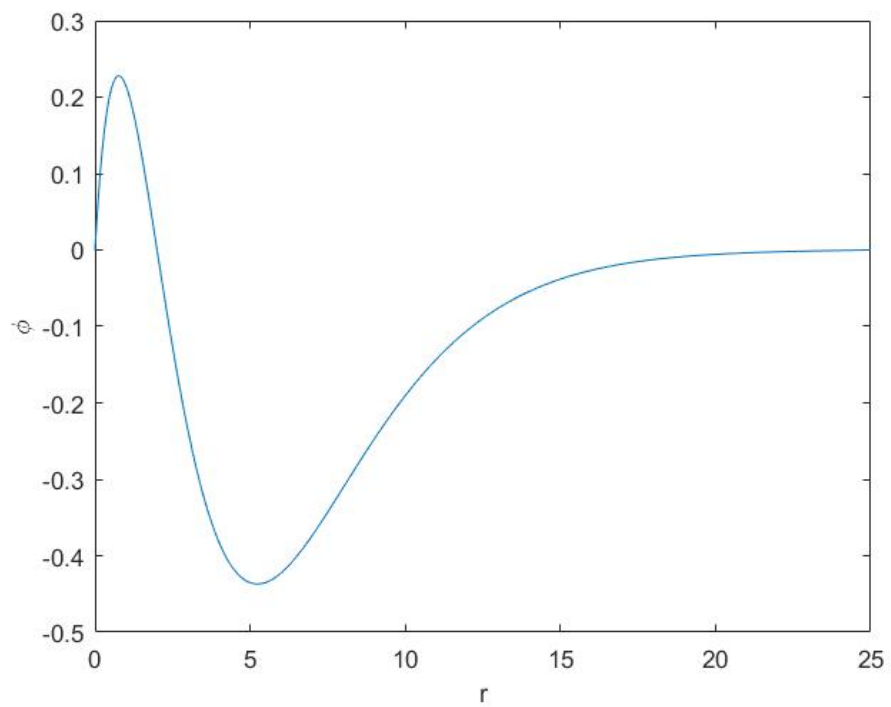
**Figure 5.2:** Eigenfunction for the 1s orbital and its corresponding energy eigenvalue with $\varepsilon = -0.2498$.

**Figure 5.3:** Eigenfunction for the 1s orbital and its corresponding energy eigenvalue with $\varepsilon = -0.1111$.

**Figure 5.4:** Eigenfunction for the 1s orbital and its corresponding energy eigenvalue with $\varepsilon = -0.0625$.

**Table 5.1:** Viable match points along with their initial guess energies and energy eigenfunctions produced.

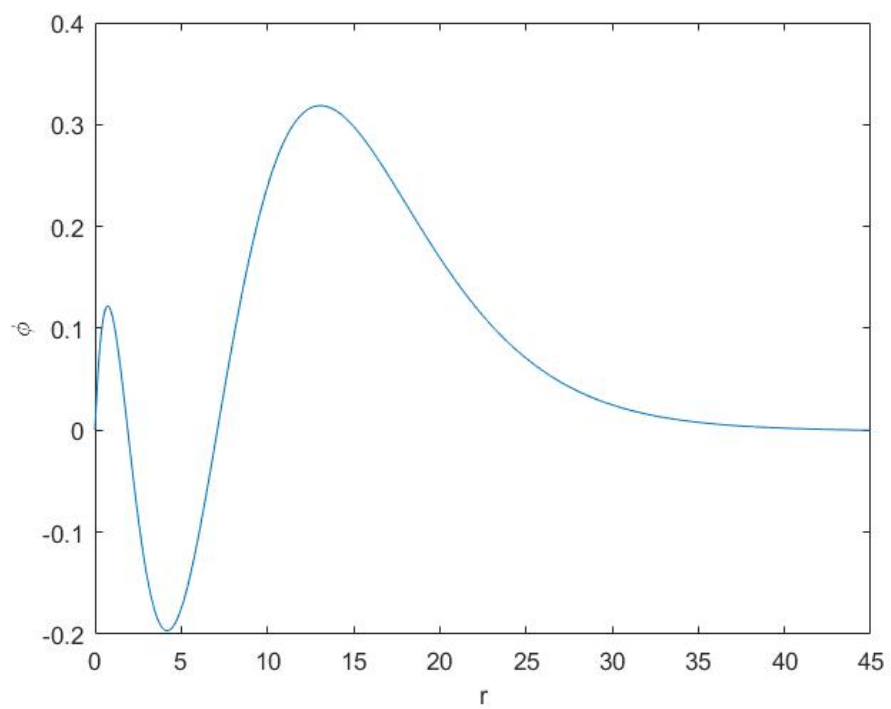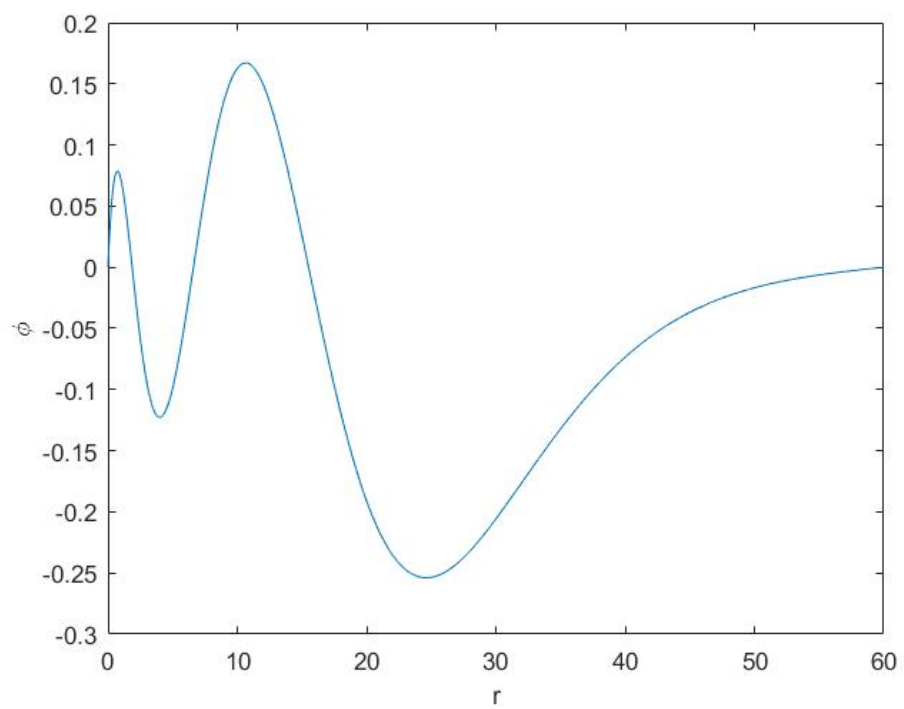| $E_{B_0}$ | Match | | | | | | | | |
|---|---|---|---|---|---|---|---|---|---|
| | 1.0 | 1.1 | 1.2 | 1.3 | 1.4 | 1.5 | 1.6 | 1.7 | 1.8 |
| -0.9 | 1s | 1s | 1s | 1s | 1s | 1s | 1s | 1s | 1s |
| -0.6 | 1s | 1s | 1s | 1s | 1s | 1s | 1s | 1s | 1s |
| -0.4 | 1s | 1s | 1s | 1s | 1s | 1s | 1s | 1s | 1s |
| -0.37 | 1s | 1s | 1s | 1s | 1s | 1s | 1s | 1s | 1s |
| -0.36 | 2s | 1s | 1s | 1s | 1s | 1s | 1s | 1s | 1s |
| -0.35 | 2s | 1s | 1s | 1s | 1s | 1s | 1s | 1s | 1s |
| -0.34 | 2s | 2s | 1s | 1s | 1s | 1s | 1s | 1s | 1s |
| -0.33 | 2s | 2s | 2s | 1s | 1s | 1s | 1s | 1s | 1s |
| -0.32 | 2s | 2s | 2s | 1s | 1s | 1s | 1s | 1s | 1s |
| -0.31 | 2s | 2s | 2s | 2s | 1s | 1s | 1s | 1s | 1s |
| -0.3 | 2s | 2s | 2s | 2s | 2s | 1s | 1s | 1s | 1s |
| -0.29 | 2s | 2s | 2s | 2s | 2s | 2s | 1s | 1s | 1s |
| -0.28 | 2s | 2s | 2s | 2s | 2s | 2s | 2s | 1s | 1s |
| -0.27 | 2s | 2s | 2s | 2s | 2s | 2s | 2s | 2s | 1s |
| -0.26 | 2s | 2s | 2s | 2s | 2s | 2s | 2s | 2s | 2s |
| -0.23 | 2s | 2s | 2s | 2s | 2s | 2s | 2s | 2s | 2s |
| -0.2 | 2s | 2s | 2s | 2s | 2s | 2s | 2s | 2s | 2s |
| -0.18 | 2s | 2s | 2s | 2s | 2s | 2s | 2s | 2s | 2s |
| -0.14 | 2s | 2s | 2s | 2s | 2s | 2s | 2s | 2s | 2s |
| -0.13 | 3s | 3s | 3s | 2s | 2s | 2s | 2s | 2s | 2s |
| -0.12 | 3s | 3s | 3s | 3s | 3s | 3s | 2s | 2s | 2s |
| -0.11 | 3s | 3s | 3s | 3s | 3s | 3s | 3s | 3s | 3s |
| -0.1 | 3s | 3s | 3s | 3s | 3s | 3s | 3s | 3s | 3s |
| -0.09 | 3s | 3s | 3s | 3s | 3s | 2s | 2s | 2s | 1s |
| -0.07 | 4s | 4s | 4s | 3s | 3s | 2s | 3s | 2s | 3s |
| -0.069 | 4s | 3s | 3s | 4s | 3s | 2s | 3s | 2s | 2s |
| -0.066 | 4s | 4s | 4s | 4s | 3s | 2s | 3s | 2s | 2s |
| -0.064 | 4s | 4s | 4s | 4s | 4s | 4s | 4s | 4s | 1s |
| -0.063 | 4s | 4s | 4s | 4s | 4s | 4s | 4s | 4s | 4s |
| -0.0625 | 4s | 4s | 4s | 4s | 4s | 4s | 4s | 4s | 4s |
| -0.062 | 4s | 4s | 4s | 4s | 4s | 4s | 4s | 4s | 4s |
| -0.061 | 4s | 4s | 4s | 4s | 4s | 4s | 4s | 4s | 1s |
| -0.06 | 4s | 4s | 4s | 4s | 4s | 4s | 4s | 1s | 1s |

# Chapter 6

# CALCULATE THE SCATTERING AND BOUND STATE SOLUTIONS USING AN AMPUTATED WAVE FUNCTION

## 6.1  Overview

Now we examine the HF technique used by Hahn and Zerrad [67] simultaneously applied to the bound and scattering states whose solutions are inter-dependent. In Chapter 2, solving for the scattering state wave equation by using a known bound function was discussed in detail. This chapter will show how to apply a similar method to solve for the bound state wave equation. Only the homogeneous equations will be solved, and this will allow the numerical method from the Chapters 3 and 5 to be used to solve for the wave equations.

## 6.2  Creating the Amputated Function to Solve for the Bound State Wave Function for Positron-Hydrogen

In this section, we introduce a method to find the bound state equation in terms of the scattering equation. Recall the following positron-hydrogen equation for Chapter 2,

$$\left[ -\bigtriangledown^2_{\mathbf{r}_1} - \bigtriangledown^2_{\mathbf{r}_2} - \frac{2}{\mathbf{r}_1} + \frac{2}{\mathbf{r}_2} - \frac{2}{\mathbf{r}_{12}} - E_C - E_B \right] \Psi(\mathbf{r}_1, \mathbf{r}_2) = 0. \tag{6.1}$$

The Hartree Fock approximation in lowest order without exchange terms is

$$\Psi(\mathbf{r}_1, \mathbf{r}_2) = \phi(\mathbf{r}_1)\psi(\mathbf{r}_2), \tag{6.2}$$

and given a potential function for $\psi$ is determined. Asymptotically, $\psi$ behaves as

$$\frac{\sin(kr_2)}{r_2} + \tan \delta^0 \frac{\cos(kr_2)}{r_2}. \tag{6.3}$$

If an attempt is made to construct a set of equations, we would have

$$< \Psi | \Psi > = < \psi | \psi > \to \infty. \tag{6.4}$$

In order to solve for the bound state wave function, the scattering wave function $\psi$ must be amputated due to its lack of integrability. The amputated function is constructed as follows: Let

$$X(\mathbf{r}_2) = V(\mathbf{r}_2)\psi(\mathbf{r}_2). \tag{6.5}$$

The scattering wave function $\psi$ will be replaced by the amputated wave function $X$. Then the Hartree Fock approximation is applied to (6.1). Multiply by $X(\mathbf{r}_2)$ on the left and integrating with respect to $\mathbf{r}_2$ yields

$$\int X(\mathbf{r}_2) \left\{ -\nabla_{\mathbf{r}_1}^2 - \nabla_{\mathbf{r}_2}^2 - \frac{2}{\mathbf{r}_1} + \frac{2}{\mathbf{r}_2} - \frac{2}{\mathbf{r}_{12}} - E_C - E_B \right\} \phi(\mathbf{r}_1)\psi(\mathbf{r}_2)d^3\mathbf{r}_2 = 0. \tag{6.6}$$

Rewrite the integral as

$$\int X(\mathbf{r}_2) \left\{ -\nabla_{\mathbf{r}_1}^2 - \frac{2}{\mathbf{r}_1} + \frac{2}{\mathbf{r}_{12}} - E_B \right\} \phi(\mathbf{r}_1)\psi(\mathbf{r}_2)d^3\mathbf{r}_2$$
$$+ \int X(\mathbf{r}_2) \left\{ -\nabla_{\mathbf{r}_2}^2 - \frac{2}{\mathbf{r}_2} - E_C \right\} \phi(\mathbf{r}_1)\psi(\mathbf{r}_2)d^3\mathbf{r}_2 = 0. \tag{6.7}$$

Then we have

$$\left\{ -\nabla_{\mathbf{r}_1}^2 + V_X(\mathbf{r}_1) - E_B - \frac{\left\langle X(\mathbf{r}_2) \middle| E_C + \nabla_{\mathbf{r}_2}^2 \middle| \psi(\mathbf{r}_2) \right\rangle_{\mathbf{r}_2}}{\left\langle X(\mathbf{r}_2) | \psi(\mathbf{r}_2) \right\rangle_{\mathbf{r}_2}} + \left\langle X(\mathbf{r}_2) \middle| -\frac{2}{\mathbf{r}_2} \middle| \psi(\mathbf{r}_2) \right\rangle_{\mathbf{r}_2} \right\} \phi(\mathbf{r}_1) = 0. \tag{6.8}$$

where

$$\left\langle X | X \right\rangle_{\mathbf{r}_2} = \frac{\left\langle X(\mathbf{r}_2) \middle| E_C + \nabla_{\mathbf{r}_2}^2 \middle| \psi(\mathbf{r}_2) \right\rangle_{\mathbf{r}_2}}{\left\langle X(\mathbf{r}_2) \middle| \psi(\mathbf{r}_2) \right\rangle_{\mathbf{r}_2}} \equiv E_{XX} \tag{6.9}$$

and

$$V_X \rightarrow E_X \equiv \left\langle X(\mathbf{r}_2) \middle| - \frac{2}{\mathbf{r}_2} \middle| \psi(\mathbf{r}_2) \right\rangle_{\mathbf{r}_2}. \tag{6.10}$$

The potential is $V_X(\mathbf{r}_1)$

$$V_X(\mathbf{r}_1) = -\frac{2}{\mathbf{r}_1} + \frac{B}{A} \tag{6.11}$$

where

$$A = \left\langle X(\mathbf{r}_2) \middle| \psi(\mathbf{r}_2) \right\rangle$$
$$B = \left\langle X(\mathbf{r}_2) \middle| \frac{2}{\mathbf{r}_{12}} \psi(\mathbf{r}_2) \right\rangle.$$

For simplicity, the integrals are now written as constants. The equation becomes

$$\left\{ -\nabla_{r_1}^2 + V_X(r_1) - E_B - E_{XX} + \frac{E_x}{A} \right\} \phi(r_1) = 0. \tag{6.12}$$

If we add and subtract $E_X$, then write the equation as

$$\left\{ \nabla_{r_1}^2 - V_B(r_1) + E_{DT} \right\} \phi(r_1) = 0, \tag{6.13}$$

and define the strong potential $V_B$ to be

$$V_B = V_X - \frac{E_X}{A} + E_X, \tag{6.14}$$

and pseudo-false binding energy, $E_{DT}$ as

$$E_{DT} = E_B + E_{XX} - E_X. \tag{6.15}$$

These conditions are necessary to satisfy $\phi$. Even though the energy is shifted, $E_B$ should still be close to -1.

### 6.2.1  Iteration Process to Solve for Scattering Phase Shift and Bound Energy

1 Choose an arbitrary $\phi$ that is the ground state wave function (as an initial guess).

2 Use the initial ground state wave function to compute the static potential ($V^S$) for the scattering wave function.

3 Solve for the scattering wave function and corresponding phase shift based on the potential computed and desired scattering energy.

4 Compute the amputated function based off the potential energy and the scattering wave function.

5 Evaluate the bound potential, $V_B$ and approximate the puesdo false energy, $E_{DT}$.

6 The binding energy $E_B$ is found by solving for (6.15).

7 The phase shift and binding energy are compared with the previous iteration. This process is repeated until the change in $E_B$ and $\delta$ are below a certain threshold.

### 6.3  Numerical Results

Figures 6.1, 6.2, 6.3, and 6.4 show the amputated function computed for different quantum states up to $n = 4$. These amputated functions where used to compute the bound state

with the effects of the scattering state. Tables 6.1, 6.2, 6.3, and 6.4 show all possible scattering states that yield accurate eigenvalue energies and eigenfunctions. Adding the effects of the scattering state does effect the energy eigenvalue of the bound state. As continuum energy increased ($E_C > 0.1$), the accuracy of the eigenvalue energy diminished.
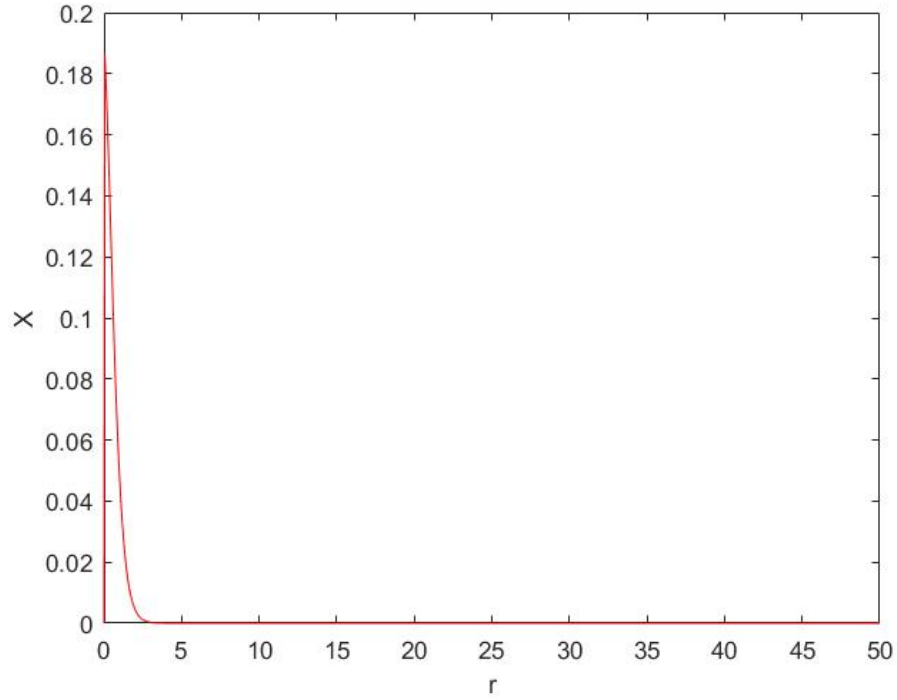
**Figure 6.1:** Plot of the amputated function for the 1s for $E_C = 0.02$.

**Table 6.1:** The phase shifts for a scattering wave functions without exchange and their corresponding energies.

| $\varepsilon_0 = -0.9$ | | |
|---|---|---|
| $E_C$ | $\varepsilon$ | $\delta$ |
| 0.1 | -0.9807 | -0.0997 |
| 0.08 | -0.9807 | -0.0898 |
| 0.06 | -0.9807 | -0.0782 |
| 0.05 | -0.9807 | -0.7166 |
| 0.04 | -0.9807 | -0.0643 |
| 0.03 | -0.9807 | -0.0559 |
| 0.02 | -0.9807 | -0.0458 |
| 0.01 | -0.9807 | -0.0325 |

**Figure 6.2:** Plot of the amputated function for the 2s for $E_C = 0.02$.

**Table 6.2:** The phase shifts for a scattering wave functions without exchange and their corresponding energies.

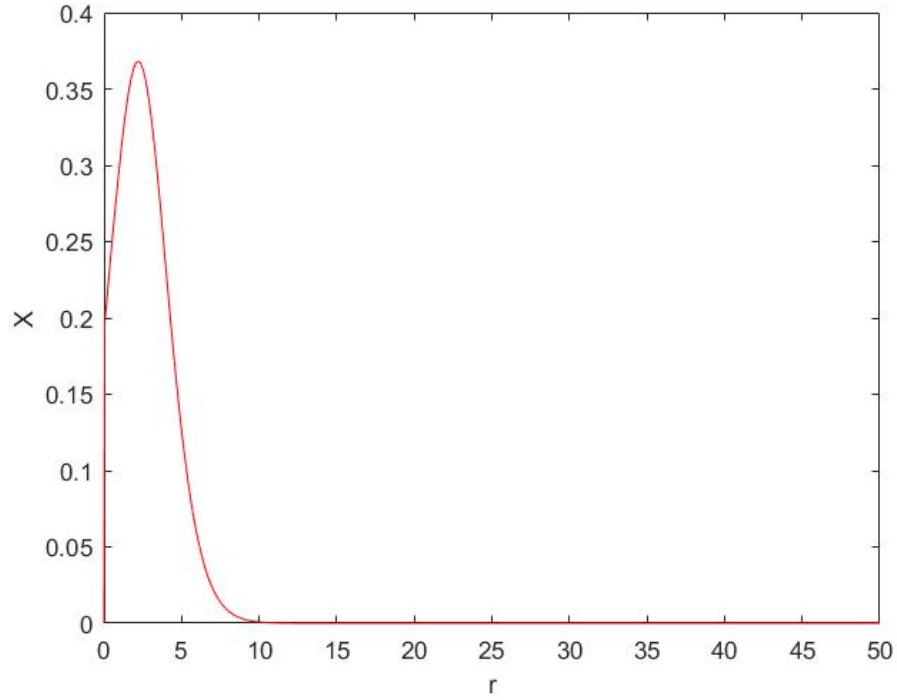| $\varepsilon_0 = -0.2$ | | |
|---|---|---|
| $E_C$ | $\varepsilon$ | $\delta$ |
| 0.1 | -0.2197 | -0.7189 |
| 0.08 | -0.2214 | -0.6602 |
| 0.06 | -0.2231 | -0.5877 |
| 0.05 | -0.2240 | -0.5442 |
| 0.04 | -0.2249 | -0.4939 |
| 0.03 | -0.2258 | -0.4342 |
| 0.02 | -0.2267 | -0.3600 |
| 0.01 | -0.2276 | -0.2586 |

**Figure 6.3:** Plot of the amputated function for the 3s for $E_C = 0.02$.

**Table 6.3:** The phase shifts for a scattering wave functions without exchange and their corresponding energies.

| $\varepsilon_0 = -0.09$ | | |
|---|---|---|
| $E_C$ | $\varepsilon$ | $\delta$ |
| 0.1 | -0.0939 | -1.753 |
| 0.08 | -0.0956 | -1.655 |
| 0.06 | -0.0975 | -1.520 |
| 0.05 | -0.0984 | -1.432 |
| 0.04 | -0.0995 | -1.323 |
| 0.03 | -0.1005 | -1.186 |
| 0.02 | -0.1016 | -1.004 |
| 0.01 | -0.1027 | -0.7377 |
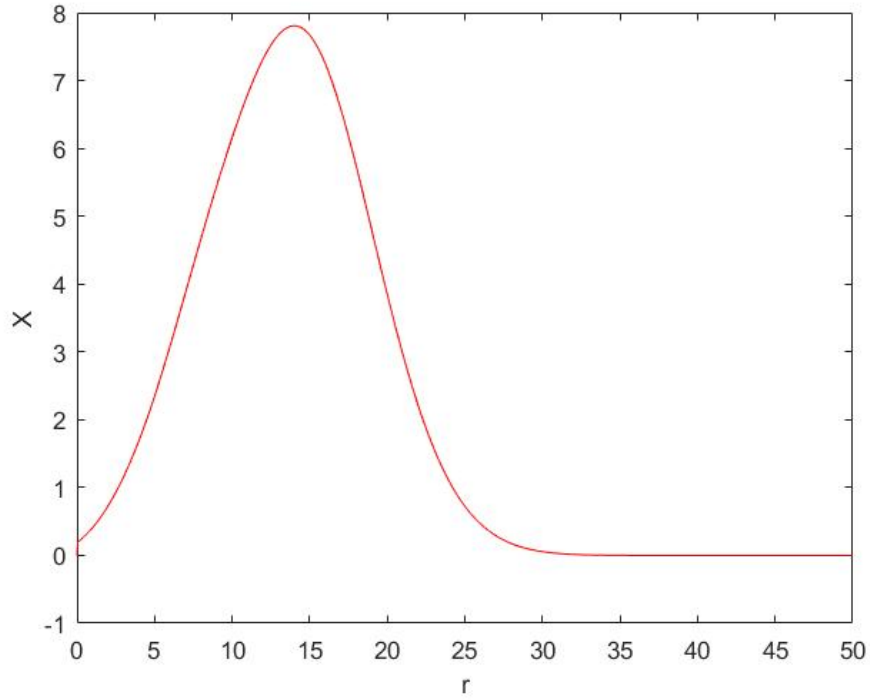
**Figure 6.4:** Plot of the amputated function for the 4s for $E_C = 0.02$.

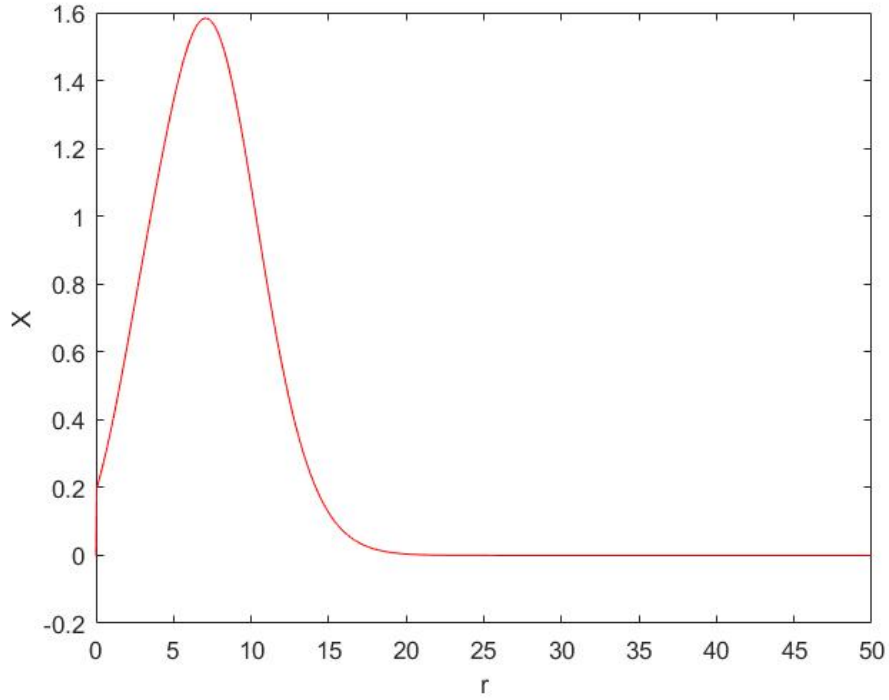**Table 6.4:** The phase shifts for a scattering wave functions without exchange and their corresponding energies.

| $\varepsilon_0 = -0.06$ | | |
|---|---|---|
| $E_C$ | $\varepsilon$ | $\delta$ |
| 0.1 | -0.0501 | -2.849 |
| 0.08 | -0.0513 | -2.771 |
| 0.06 | -0.0528 | -2.637 |
| 0.05 | -0.0537 | -2.535 |
| 0.04 | -0.0546 | -2.396 |
| 0.03 | -0.0564 | -2.203 |
| 0.02 | -0.0567 | -1.918 |
| 0.01 | -0.0579 | -1.455 |

# Chapter 7

# CONCLUSION

The HFA theory was reviewed to show how the self consistent field approach can be applied to an atomic system with many electrons. This methodology was applied to hydrogenic atomic systems (positron-hydrogen and electron-hydrogen) to solve for the scattering and bound wave equations.

We employed three numerical techniques to solve for the scattering wave function. Numerov was applied to discretize the equations along with the boundary conditions. This method was successful for positron-hydrogen scattering and the triplet case for electron-scattering. The rate of convergence for the triplet was less efficient as the energies decreased. For the singlet case, this method failed to converge for any energy ($E_C$). The Green's function method was only successful for certain energies for the singlet and triplet cases. Convergence improved as the energy was lowered. Using the SVD Method yields convergence for all energy levels tested for the singlet and triplet case. The rate of convergence was improved significantly. All energies tested converged in less than 5 iterations for the SVD method.

When applying the Green's Function methods, two key adjustments were implemented: (i) computing the Wronskian when constructing computing the Green's function for both methods and (ii) for the SVD, the Green's function that only includes the affect of the potential ($G_V$) which acts on the remainder matrix $K_r$. By making these changes, the rate of convergence as well as the amount of low energies converging improved.

The energy matching method was applied to solve for the bound state energies and wave functions with an acceptable level of accuracy. The rate of convergence is dependent on the match selected and how far the initial guess is from the actual solution. The solution

was not reliable when the spatial step was lowered to achieve a more accurate solution.

Convergence was achieved when the scattering and bound states were solved simultaneously for positron-hydrogen. Computing and applying the amputated function to solve for the scattering wave function was successful in treating the nonintegrablity of the scattering states for $E_c \leq 0.1$.

In conclusion, we were able to employ several numerical methods successfully for scattering and bound states. We were able to improve the SVD method for electron-hydrogen scattering to solve singlet and triplet cases for a wide range of lower energies via a self-consistent field.

# Chapter 8

# FUTURE WORK

## 8.1 Overview

In the future, we plan to use the a HF technique used by Hahn and Zerrad [67] simultaneously applied to the bound and scattering states whose solutions are inter-dependent for electron-hydrogen. In Chapter 2, solving for scattering state wave equation by using a known bound function was discussed in detail. In this chapter, a similar methodology that was applied in chapter 6 is developed used to solve electron hydrogen bound state wave equation. The numerical methods from the Chapters 4 and 5 are to be used to solve for the wave equations.

## 8.2 Creating the Amputated Function to Solve for the Bound State Wave Function for Electron-Hydrogen

In order to create a amputated function to solve for the bound state, we must find the scattering state for electron-hydrogen. These equations were derived in Chapter 2. The scattering ordinary differential equation with exchange terms is

$$\left[ \nabla_{r_2}^2 - V_S(r_2) + E_C \right] \psi(r_2) \ = \ \pm \frac{1}{A} \left[ (E_B - E_C)C + D \right] \phi(r_2) \tag{8.1}$$

and the potential is

$$V_S(r_1) = -\frac{2}{r_1} + \frac{B}{A}. \tag{8.2}$$

For simplicity, label the right hand side of the scattering equation, $K_\psi$. The amputated function for electron-hydrogen is

$$X(r_2) = \left[V^S(r_2) \pm K_\psi\right]\psi(r_2). \tag{8.3}$$

Now, that a solution for the scattering wave function $\psi$ is found, the scattering solution is amputated. This is executed by multiplying the scattering function by the potential found in (8.2). The amputated wave function for the scattering will be labeled as $X$. The amputated wave function replaces the scattering wave function $\psi$ in the HFA. The HFA is applied to the total wave function by multiplying by the amputated wave function $X(r_1)$. Integrating with respect to $r_1$, will yield

$$\int X(\mathbf{r}_1)\left[-\nabla_{\mathbf{r}_1}^2 - \nabla_{\mathbf{r}_2}^2 - \frac{2}{\mathbf{r}_1} - \frac{2}{\mathbf{r}_2} + \frac{2}{\mathbf{r}_{12}} - E_C - E_B\right][\psi_i(\mathbf{r}_1)\phi_i(\mathbf{r}_2)$$
$$\pm\psi_i(\mathbf{r}_2)\phi_i(\mathbf{r}_1)]\,d^3\mathbf{r}_2 = 0 \tag{8.4}$$

or

$$I_3 \pm I_4 = 0 \tag{8.5}$$

Here, the integral is split, and $I_3$ is evaluated. Rewrite the integral as

$$\begin{aligned}
I_3 &= \int X(\mathbf{r}_1)\left\{-\nabla_{\mathbf{r}_2}^2 - \frac{2}{\mathbf{r}_2} + \frac{2}{\mathbf{r}_>} - E_B\right\}\psi(\mathbf{r}_1)\phi(\mathbf{r}_2)d^3\mathbf{r}_1 \\
&+ \int X(\mathbf{r}_1)\left\{-\nabla_{\mathbf{r}_1}^2 - \frac{2}{\mathbf{r}_1} - E_C\right\}\psi(\mathbf{r}_1)\phi(\mathbf{r}_2)d^3\mathbf{r}_1.
\end{aligned} \tag{8.6}$$

Then we have

$$I_3 = \left\{ -\nabla_{\mathbf{r}_2}^2 + V_X(\mathbf{r}_2) - E_B - \frac{\left\langle X(\mathbf{r}_1) \middle| E_C + \nabla_{\mathbf{r}_1}^2 \middle| \psi(\mathbf{r}_1) \right\rangle_{\mathbf{r}_1}}{\left\langle X(\mathbf{r}_1) | \psi(\mathbf{r}_1) \right\rangle_{\mathbf{r}_1}} + \left\langle X(\mathbf{r}_1) \middle| -\frac{2}{\mathbf{r}_1} \middle| \psi(\mathbf{r}_1) \right\rangle_{\mathbf{r}_1} \right\} \phi(\mathbf{r}_2).$$

$$(8.7)$$

where

$$\left\langle X | X \right\rangle_{\mathbf{r}_1} = \frac{\left\langle X(\mathbf{r}_1) \middle| E_C + \nabla_{\mathbf{r}_1}^2 \middle| \psi(\mathbf{r}_1) \right\rangle_{\mathbf{r}_1}}{\left\langle X(\mathbf{r}_1) \middle| \psi(\mathbf{r}_1) \right\rangle_{\mathbf{r}_1}} \equiv E_{XX} \qquad (8.8)$$

and

$$V_X \to E_X \equiv \left\langle X(\mathbf{r}_1) \middle| -\frac{2}{\mathbf{r}_1} \middle| \psi(\mathbf{r}_1) \right\rangle_{\mathbf{r}_1}. \qquad (8.9)$$

The potential $V_X(\mathbf{r}_2)$ is

$$V_X(\mathbf{r}_2) = -\frac{2}{\mathbf{r}_2} + \frac{E}{F} \qquad (8.10)$$

and

$$E = \left\langle X(\mathbf{r}_1) \middle| \psi(\mathbf{r}_1) \right\rangle$$
$$F = \left\langle X(\mathbf{r}_1) \middle| \frac{2}{\mathbf{r}_{12}} \psi(\mathbf{r}_1) \right\rangle.$$

The strong potential to solve the for $\phi$ is

$$V_B = V_X - \frac{E_X}{E} + E_X, \qquad (8.11)$$

and the puesdo energy is

$$E_{DT} = E_B + E_{XX} - E_X. \qquad (8.12)$$

Hence,

$$I_3 = \left[\nabla^2_{\mathbf{r}_2} - V_B(\mathbf{r}_2) + E_{DT}\right]\phi(\mathbf{r}_2). \tag{8.13}$$

Now, $I_4$ is split into a separate integral. It is assumed that

$$\int X(\mathbf{r}_1)\left\{-\nabla^2_{\mathbf{r}_1} - \frac{2}{\mathbf{r}_1} - E_B\right\}\psi(\mathbf{r}_2)\phi(\mathbf{r}_1)d^3\mathbf{r}_1 = 0.$$

Then, we obtain

$$
\begin{aligned}
I_4 &= \int X(\mathbf{r}_1)\left\{-\nabla^2_{\mathbf{r}_1} - \nabla^2_{\mathbf{r}_2} - \frac{2}{\mathbf{r}_1} - \frac{2}{\mathbf{r}_2} + \frac{2}{\mathbf{r}_{12}} - E_C - E_B\right\}\psi(\mathbf{r}_2)\phi(\mathbf{r}_1)d^3\mathbf{r}_1 \\
&= \int X(\mathbf{r}_1)\left\{-\nabla^2_{\mathbf{r}_1} - \frac{2}{\mathbf{r}_1} - E_B\right\}\psi(\mathbf{r}_2)\phi(\mathbf{r}_1)d^3\mathbf{r}_1 \\
&\quad + \int X(\mathbf{r}_1)\left\{-\nabla^2_{\mathbf{r}_2} - \frac{2}{\mathbf{r}_2} - E_C\right\}\psi(\mathbf{r}_2)\phi(\mathbf{r}_1)d^3\mathbf{r}_1 \\
&\quad + \int X(\mathbf{r}_1)\left\{\frac{2}{\mathbf{r}_{12}}\right\}\psi(\mathbf{r}_2)\phi(\mathbf{r}_1)d^3\mathbf{r}_2 \\
&= \left\{\left\langle X(\mathbf{r}_1)\left|\frac{2}{\mathbf{r}_{12}}\phi(\mathbf{r}_1)\right\rangle + \left(-\nabla^2_{\mathbf{r}_2}\psi - \frac{2}{\mathbf{r}_2} - E_C\right)\left\langle x(\mathbf{r}_1)|\phi(\mathbf{r}_1)\right\rangle\right\}\psi(\mathbf{r}_2) \tag{8.14} \\
I_4 &= \left\{H + \left(-\nabla^2_{\mathbf{r}_2}\psi - \frac{2}{\mathbf{r}_2} - E_C\right)G\right\}\psi(\mathbf{r}_2) \tag{8.15}
\end{aligned}
$$

where

$$
\begin{aligned}
G &= \left\langle X(\mathbf{r}_1)\middle|\phi(\mathbf{r}_1)\right\rangle \\
H &= \left\langle X(\mathbf{r}_1)\middle|\frac{2}{\mathbf{r}_{12}}\phi(\mathbf{r}_1)\right\rangle.
\end{aligned}
$$

Hence, we obtain

$$\left[\nabla^2_{r_2} - V_B(r_2) + E_{DT}\right]\phi(r_2) = \pm\frac{1}{E}\left\{H + \left(-\nabla^2_{r_2}\psi - \frac{2}{r_2} - E_C\right)G\right\}\psi(r_2). \tag{8.16}$$

71

The iteration process is the same as in section 6.2.1.

Solutions to this problem have been attempted. We believe that due to the sensitivity of the energy matching method, it causes the bound state wave function to be divergent. We will continue to investigate this method.

# REFERENCES

[1] Anastassi, Z. A., Vlachos, D. S., Simos, T. E. (2009). "A New Methodology for the Development of Numerical Methods for the Numerical Solution of the Schrödinger Equation." *Journal of Mathematical Chemistry.* **46**: 621 - 651.

[2] Arellano, H. F., Blanchon, G. (2019)." Exact scattering waves off nonlocal potential under Coulomb interaction within Schrödinger's Integro-Differential Equation." *Physics Letters B.* **789**: 256 - 261.

[3] Arfken, G. B., Weber, H. J. (2005). <u>Mathematical Methods for Physicists</u>. Elsevier Academic Press.

[4] Armour, E. A. G., Humberston, J. W. (1991). "Methods and Programs in Collisions of Positrons with Atoms and Molecules." *Physics Reports.* **204**: 165 - 251.

[5] Berghe, G. V., Fack, V., De Meyer, H. E. (1989). "Numerical Methods for Solving Radial Schrödinger Equations." *Journal of Computational and Applied Mathematics.* **28**: 391 - 401.

[6] Botero, J., Sherzter, P. G.(1992). "Direct Numerical Solution of the Schrödinger Equation for Quantum Scattering Problems." *Physical Review A.* **46**: R1155 - R1158.

[7] Bransden, B. H., Dalgarno, A., John, T. L., Seaton, M. J., (1958). "The Elastic Scattering of Slow Electrons by Hydrogen Atoms." *Proceedings of the Physical Society.* **71**: 877 - 892.

[8] Brown, G.E., Gunn, J.H., Gould, P. (1963). "Effective Mass in Nuclei." *Nuclear Physics.* **46**: 598 - 606.

[9] Bray, I., Stelbovics, A. T. (1992). "Convergent Close-Coupling Calculations of Electron-Hydrogen Scattering." *Physical Review A.* **46**: 6995 - 7011.

[10] Bray, I. (1994). "Convergent Close-Coupling Method for the Calculation of Electron Scattering on Hydrogen-like Targets." *Physical Review A.* **49**: 1066 - 1082.

[11] Bray, I. (1995). "The Convergent Close-Coupling Method for a Coulomb Three-Body Problem." *Computer Physics Communications.* **85**: 1 - 17.

[12] Burke, P. G.(1963). "The Convergence of the Close Coupling Expansion." *Proceedings of the Physical Society.* **82**: 443 - 445.

[13] Burke, P. G., Schey, H. M., Smith, K. (1963). "Collisions of Slow Electrons and Positrons with Atomic Hydrogen." *Physical Review.* **129**: 1258 - 1274.

[14] Burke, P. G., Ormonde, S., Whitaker, W. (1967). "Low-Energy Electron Scattering by Atomic Hydrogen: I. The Close-Coupling Approximation." *Proceedings of the Physical Society.* **92**: 319 - 335.

[15] Burke, P. G., Robb, W. D. (1971). "Elastic Scattering of Electrons by Hydrogen and Helium." *Journal of Physics B: Atomic, Molecular, and Optical Physics.* **5**: 44 - 54.

[16] Burke, P. G., Scott (1987). "R-matrix Theory of Electron Scattering at Intermediate Energies." *Proceedings of the Royal Society of London.* **410**: 289 - 310.

[17] Čertík, O., Pask, J. (2013). " dftatom: A Robust and General Schrödinger and Dirac Solver for Atomic Structure Calculations." *Computer Physics Communications.* **184**: 1777 - 1791.

[18] Chang, S. (1990). Introduction to Quantum Field Theory. World Scientific Publishing Co. Pte. Ltd.

[19] Falconer, I. (2001). "Corpuscles to Electrons in J Buchwald and A Warwick, Histories of the Electron." *Cambridge, Mass: MIT Press*, 77 - 100.

[20] Fonte, G., Mignani, R., Schiffrer, G. (1948). "Solution of the Hartree-Fock Equations." *Communications in Mathematical Physics.* **33**: 293 - 304.

[21] Friedrich, H. (1991). Theoretical Atomic Physics. Springer-Verlag.

[22] Friedrich, H. (2013). Scattering Theory. Springer.

[23] Frocese Fisher, C. (1977). The Hartree-Fock Method for Atoms: A Numerical Approach. Wiley New York.

[24] Froese Fischer, C. (2003). Douglas Rayner Hartree: His Life in Science and Computing. World Scientific Publishing Company Pte. Ltd.

[25] Griffriths, R. B. (2002). Consistent Quantum Theory. Cambridge University Press.

[26] Hahn, Y. (1996). "Generalized Hartree and Hartree-Fock Approaches for Atomic Collisions." *Journal of Physics B: Atomic, Molecular and Optical Physics.* **29**: 1385 - 1396.

[27] Hahn, Y. (1997). "Generalization of the Hartree-Fock Approach to Collision Process." *Physical Review A.* **55**: 4238 - 4243.

[28] Hahn, Y. (2014). "Self-Consistent Field Theory of Collisions: Orbital Equations with Asymptotic Sources and Self-Averaged Potentials." *Annuals of Physics.* **351**: 857 - 871.

[29] Hartree, D. (1928). "The Wave Mechanics of an Atom with a Non-Coulomb Central Field. Part I. Theory and Methods." *Mathematical Proceedings of the Cambridge Philosophical Society.* **24**: 89 - 110.

[30] Hartree, D. (1928). "The Wave Mechanics of an Atom with a Non-Coulomb Central Field. Part II. Some Results and Discussion." *Mathematical Proceedings of the Cambridge Philosophical Society.* **24**: 111 - 132.

[31] Heath, M. T. (2011). Scientific Computing; An Introductory Survey. Tata McGraw-Hill.

[32] Hylleraas, E. A. (1929)." Neue Berechnung der Energie des Heliums im Grundzustande, sowie des tiefsten Terms von Ortho-Helium." *Z. Physics* **54**: 347 - 366.

[33] Ixaru, L.G., Rizea, M. (1980). "A Numerov-like scheme for the numerical solution of the Schrödinger Equation in the Deep Continuum Spectrum of Energies." *Computer Physics Communication.* **19**: 23 - 27.

[34] John, T. L. (1960). "The Numerical Solution of the Exchange Equations for Slow Electron Collisions with Hydrogen Atoms." *Proceedings of the Physical Society.* **76**: 532 - 538.

[35] Kantorovich, L. V. (1948). "Functional Analysis and Applied Mathematics." *Uspekhi Mat. Nauk.* **3**: 89185.

[36] Kim, B. T., Udagawa, P. G. (1990). "Method for nonlocal optical model calculations." *Physical Review C.* **42**: 1147 - 1149.

[37] Lanczos, C. (1950). "An Iteration Method for the Solution of the Eigenvalue Problem of Linear Differential and Integral Operators." *Journal of Research of the National Bureau of Standards.* **45**: 255 - 282.

[38] Lieb, E., Simon, B. (1977). "The Hartree-Fock theory for Coulomb systems." *Communications in Mathematical Physics.* **53**: 185 194.

[39] Lyche (1972)."Chebyshevian Multistep Methods for Ordinary Differential Equations." *Numerische Mathematik.* **19**: 65 - 75.

[40] Nikolopoulos, L. (2013). "Calculation Method for the Continuum States of Atomic Systems."*Central European Journal of Physics.* **11**: 1074 -1081.

[41] Pillai, M., Goglio, J., Walker, T. G., (2012). "Matrix Numerov Method for Solving Schrödinger's Equation." *American Journal of Physics.* **80**: 1017 - 1019.

[42] Poet, R. (1978). "The Exact Solution for a Simplified Model of Electron Scattering by Hydrogen Atoms." *Journal of Physics B: Atomic and Molecular Physics.* **11**: 3081 - 3094.

[43] Poet, R. (1980). "Symmetrically coupled partial differential equations in scattering. I. Model electron-hydrogen collisions." *Journal of Physics B: Atomic and Molecular Physics.* **13**: 2995 - 3008.

[44] Quiroz Gonzalez, J. L. M., Thompson, D. (1997). "Getting Started with Numerov's Method." *Computers in Physics.* **11**: 514 - 515.

[45] Raptis, A. D., Allison, A.C. (1978). "Exponential-fitting Methods for the Numerical Solution of the Schrödinger Equation." *Computer Physics Communication.* **14**: 1 - 5.

[46] Raptis, A. D. (1981). "On the Numerical Solution of the Schrödinger Equation." *Computer Physics Communications.* **24**: 1 - 4.

[47] Ratwitscher, G. H., Kang, S. Y., Koltracht, I. (2003). "A Novel Method for the Solution of the Schrödinger Equation in the Presence of Exchange Terms." *The Journal of Chemical Physics.* **118**: 9149 - 9156.

[48] Salvat, F., Frenández-Varea, J., Williamson,W. (1995). "Computer Programs in Physics Accurate Numerical Solution of the Radial Schrödinger and Dirac Wave Equations." *Computer Physics Communications.* **90**: 151 - 168.

[49] Salvat, F., Frenández-Varea, J. (2019) "RADIAL: A Fortran Subroutine Package for the Solution of the Radial Schrödinger and Dirac Wave Equations." *Computer Physics Communications.* **240**: 165 - 177.

[50] Sams, W. N., Kouri, D. J. (1969). "Noniterative Solutions of Integral Equations for Scattering. I. Single Channels." *The Journal of Chemical Physics.* **51**: 4809 - 4814.

[51] Sams, W. N., Kouri, D. J. (1969). "Noniterative Solutions of Integral Equations for Scattering. II. Coupled Channels." *The Journal of Chemical Physics.* **51**: 4815 - 4819.

[52] Scholz, T., Burke, P. G. (1988). "Electron-Hydrogen Atom Scattering at Intermediate Energies." *Journal of Physics B: Atomic, Molecular, and Optical Physics.* **21**: L139 - L145.

[53] Schwartz, C. (1961) "Electron Scattering from Hydrogen." *Physical Review.* **124**: 1468 - 1471.

[54] Scott, M. P., Burke, P. G. (1993). "Electron Scattering from Hydrogen Atoms at Intermediate Energies: Excitation to n=3 Levels." *Journal of Physics B: Atomic, Molecular, and Optical Physics.* **23**: L191 - L195.

[55] Seaton, M. J. (2002). "NUMER, a Code for Numerov Integrations of Coulomb Functions." *Computer Physics Communications.* **146**: 254 260.

[56] Shao, S., Cai, W., Tang, H. (2006). "Accurate Calculation of the Green's function of Schrödinger Equation in a Block Layered Potential." *Journal of Computational Physics.* **219**: 733 - 748.

[57] Simos, T. E. (1990). "A Four-Step Method for the Numerical Solution of the Schrödinger Equation." *Journal of Computational and Applied Mathematics.* **30**: 251 255.

[58] Simos, T. E., Tougelidis, G. (1996). "A Numerov-Type Method for Computing Eigenvalues and Resonances of the Radial Schrödinger Equation." *Computers & Chemistry.* **20**: 397 - 401.

[59] Simos, T. E. (2009). "P-stability, Trigonometric-Fitting and the Numerical Solution of the Radial Schrödinger Equation." *Computer Physics Communications.* **180**: 1072 - 1085.

[60] Simos T. E. (2009). "A New Numerov-Type Method for the Numerical Solution of the Schrödinger equation." *Journal of Mathematical Chemistry.* **46**: 981 - 1007.

[61] Slater, J. C. (1951). "A Simplification of the Hartree-Fock Method." *American Physical Society.* **81**: 385 - 390.

[62] Smith, E. R., Henry, R. J. (1973). "Noniterative Integral-Equation Approach to Scattering Problems." *Physical Review A.* **7**: 1585 - 1590.

[63] Taylor, A. J., Burke, P. G. (1967). "Low-Energy Electron Scattering by Atomic Hydrogen II. The Correlation Method." *Proceedings of the Physical Society.* **92**: 366 - 344.

[64] Waxman, D. (1998). "Numerical Determination of Bound States with Matrix Diagonalization." *Journal of Physics A: Mathematical and General.* **31**: 1329 - 1339.

[65] Wigner, E. P., Eisenbud, L. (1947). "Higher Angular Momenta and Long Range Interaction in Resonance Reactions." *American Physical Society.* **72**: 29 - 41.

[66] Vogelaere, R. (1955). "A Method for the Numerical Integration of Differential Equations of Second Order without Explicit First Derivatives." *Journal of Research of the National Bureau of Standards.* **54**: 119 - 125.

[67] Zerrad, E., Hahn, Y. (2000). "Self-consistent Field Theory of Collisions I. Scattering Channels." *The European Physical Journal D.* **10**: 81 - 97.

[68] Zerrad, E., Sameen, A., Zerrad, K., Rawitscher, G. (2003). "Singular Value Decomposition Method in Atomic Scattering." *Canadian Journal of Physics* **81**: 1215 - 1221.

[69] Zerrad, E., Triplett, R., Biswas, A. (2009). "Singular Value Decomposition Solution of the Schrödinger Equation in the Presence of Exchange Terms." *International Journal of Theoretical Physics.* **48**: 1583 - 1588.